

Rotation Curves of Spiral Galaxies

Yoshiaki SOFUE¹ and Vera RUBIN²

1. *Institute of Astronomy, University of Tokyo, Tokyo 181-0015, Japan*
2. *Department of Terrestrial Magnetism, Carnegie Institution of Wash.
5241 Broad Branch Road, N.W., Washington, DC 20015, USA*

Appeared in Ann. Rev. Astron. & Astrophys. Vol. 39, p.137, 2001

2000 October 15

Abstract

Rotation curves of spiral galaxies are the major tool for determining the distribution of mass in spiral galaxies. They provide fundamental information for understanding the dynamics, evolution and formation of spiral galaxies. We describe various methods to derive rotation curves, and review the results obtained. We discuss the basic characteristics of observed rotation curves in relation to various galaxy properties, such as Hubble type, structure, activity, and environment.

1 HISTORICAL INTRODUCTION

The rotation of galaxies was discovered in 1914, when Slipher (1914) detected inclined absorption lines in the nuclear spectra of M31 and the Sombrero galaxy, and Wolf (1914) detected inclined lines in the nuclear spectrum of M81. This evidence led Pease (1918) to use the Mt. Wilson 60-inch to “investigate the rotation of the great nebula in Andromeda” by obtaining a minor axis long slit spectrum of M31 with an exposure of 84 hours taken during clear hours in August, September, and October, 1916, and a major axis spectrum taken over 79 hours in August, September, and October, 1917. The absorption lines extended only 1.5 arcminutes in radius along the major axis, less than 2% of the optical radius, but were sufficient to show the steep nuclear velocity rise. Later studies of M31’s rotation by Babcock (1939) and Mayall (1951) extended major axis rotation velocities to almost 2° from the nucleus, but exposure times were tens of hours, and spectrographs had stability problems. Interestingly, both Babcock’s velocities for M31 and Humason’s unpublished velocities for

NGC 3115 showed the last measured point to have a rotation velocity of over 400 km s^{-1} (almost 2 times actual), but consequently raised questions of mass distribution.

At the dedication of the McDonald Observatory in 1939, Oort's (1940) comment that "...the distribution of mass [in NGC 3115] appears to bear almost no relation to that of the light" seems from the view in 2000 to have attracted little attention. His conclusion concerning the mass distribution in NGC 3115 is worth quoting, even 60 years later. "In the outer parts of the nebula the ratio f of mass density to light density is found to be very high; and this conclusion holds for whatever dynamical model we consider. The spectrum of the nebula shows the characteristics of G-type dwarfs. Since f cannot be much larger than 1 for such stars, they can account for roughly only 1/2 percent of the mass; the remainder must consist either of extremely faint dwarfs having an average ratio of mass to light of about 200 to 1 or else of interstellar gas and dust". From a reanalysis of the (scattered) velocities for M31, Schwarzschild (1954) concluded that the approximately flat rotation curve was "not discordant with the assumption of equal mass and light distribution."

The modern era of optical observations of rotation velocities within spiral galaxies dates from Page's (1952) and especially Margaret and Geoffrey Burbidge's (1960) observations which exploited the new red sensitivity of photographic plates to observe the $H\alpha$ and [NII] emission lines arising from HII regions within spiral disks. Within a decade, rotation curves existed for a few dozen galaxies, most of them extending only over the initial velocity rise and the turnover of the velocities.

Early radio observations of neutral hydrogen in external galaxies showed a slowly falling rotation curve for M31 (van de Hulst et al. 1957) and a flat rotation curve for M33 (Volders 1959). The first published velocity field ("spider diagram") was of M31 (Argyle 1965). For M33, the flatness could be attributed to the side lobes of the beam, and was consequently ignored. Louise Volders must also have realized that a flat rotation curve conflicted with the value of the Oort constants for our Galaxy, which implied a falling rotation curve at the position of the sun. Jan Oort was one of her thesis professors. By the 1970s, flat rotation curves were routinely detected (Rogstad and Shostak 1972), but worries about side bands still persisted, and a variation in M/L across the disk was a possible explanation (Roberts and Rots 1973).

Surveys of galaxy observations from these early years by de Vaucouleurs (1959) and of galactic dynamics by Lindblad (1959) reveal the development of the observations and the interpretation of the spiral kinematics. They are historically notable because they contains early references, many of which have faded into oblivion. More recent (but still early) reviews include de Vaucouleurs & Freeman (1973), Burbidge & Burbidge (1975), van der Kruit and Allen (1978).

Rotation curves are tools for several purposes: for studying the kinematics of galaxies; for inferring the evolutionary histories and the role that interactions have played; for relating departures from the expected rotation curve Keplerian form to the amount and distribution of dark matter; for observing evolution by comparing rotation curves in distant galaxies with galaxies nearby. Rotation

curves derived from emission lines such as H α , HI and CO lines are particularly useful to derive the mass distribution in disk galaxies, because they manifest the motion of interstellar gases of population I, which have much smaller velocity dispersion, of the order of 5 – 10 km s $^{-1}$, compared to the rotation velocities. This allows us to neglect the pressure term in the equation of motion for calculating the mass distribution in a sufficiently accurate approximation.

Here, we review the general characteristics of rotation curves for spiral galaxies as kinematic tracers, in relation to galaxy properties, such as Hubble types, activity, structure, and environment. These parameters are fundamental input for understanding the dynamics and mass distribution, evolution, and formation of spiral galaxies. Methods for analysis are described. In general, the discussion is restricted to studies since 1980. Higher-order, non-axisymmetric velocity components due to spiral arms and bars are not emphasized here. Although rotation curves of spiral galaxies are a major tool for determining the distribution of mass in spiral galaxies, we stress the observations rather than the mass determinations or the deconvolutions into luminous and dark matter.

Numerous discussions of rotation properties are included in the conference proceedings, *Galaxy Dynamics* (Merritt et al. 1999), *Dynamics of Galaxies* (Combes et al. 2000), *Galaxy Disks and Disk Galaxies* (Funes & Corsini 2001). Reviews of dark matter as deduced from galaxy rotation curves can be found in Trimble (1987), Ashman (1992), and Persic & Salucci (1997, and papers therein).

Spheroidal galaxies have been reviewed earlier (Faber & Gallagher 1979; Binney 1982; de Zeeuw & Franx 1991). Generally, measures of velocity and velocity dispersions are necessary for mass determinations in early type galaxies, although methods which we describe below are applicable to the cold disks often found in the cores of ellipticals, in extended disks of low-luminosity ellipticals (Rix et al. 1999), and in S0 galaxies.

Data for several million galaxies are available from huge databases accessible on the World Wide Web. Hypercat (Lyon/Meudon Extragalactic Database <http://www-obs.univ-lyon1.fr/hypercat/>) classifies references to spatially resolved kinematics (radio/optical/1-dimension/2-dim/velocity dispersion, and more) for 2724 of its over 1 million galaxies. NED (NASA/IPAC Extragalactic Database <http://nedwww.ipac.caltech.edu/index.html>) contains velocities for 144,000 galaxies. The number of measured velocity points is tabulated for each galaxy reference. Both of these sites contain extensive literature references for galaxy data. High spatial (HST) STIS spectroscopy preprints are found in <http://STScI.edu/science/preprints>.

2 THE DATA

When Margaret and Geoffrey Burbidge (1960) initiated their observational program to determine the kinematics and hence masses of spiral galaxies, they were reproducing the technique employed by Pease (1918), but with improvements. Telescopes were larger, spectrographs were faster, photographic plates were sensitive in the red. The strong emission lines of H α and [NII] could be

more easily detected and measured than the weak broad H and K absorption lines. Since the 1980s, larger telescopes and improved detectors have existed for optical, radio, and mm observations. The combination of high spatial and high spectral resolution digital detectors and speedy computers has permitted a sophistication in the velocity analyses (Section 3) that will surely continue.

2.1 H α and Optical Measurements

Optical astronomers have available several observing techniques for determining rotation curves and velocity fields for both the ionized gas and stars. Traditional long slit spectra are still valuable for deducing the rotation curve of a galaxy from emission lines (Rubin et al. 1980, 1982, 1985; Mathewson et al. 1992, 1996; Amram et al. 1992, 1994; Corradi et al. 1991; Courteau 1997; Vega Baltran 1999), but methods which return the entire velocity field, such as Fabry-Perot spectrographs (Vaughan 1989) or integral (fiber-optic) field instruments (Krabbe et al. 1997) offer more velocity information at the price of more complex and time-consuming reductions. Although H α , [NII], and [SII] emission lines have traditionally been employed, the Seyfert galaxy NGC 1068 has become the first galaxy whose velocity field has been studied from the IR [Si VI] line (Tecza et al. 2000). Distant planetary nebula (Section 2.5) and satellite galaxies are valuable test particles for determining the mass distribution at large distances from galaxy nuclei. For a limited number of nearby galaxies, rotation curves can be produced from velocities of individual HII regions in galactic disks (Rubin & Ford, 1970, 1983; Zaritsky et al. 1989, 1990, 1994).

2.2 HI line

The HI line is a powerful tool to obtain kinematics of spiral galaxies, in part because its radial extent is often greater, sometimes 3 or 4 times greater, than that of the visible disk. Bosma's thesis (1981a, b; van der Kruit & Allen 1978) played a fundamental role in establishing the flatness of spiral rotation curves. Instrumental improvements in the last 20 years have increased the spatial resolution of the beam, so that problems arising from low resolution are important only near the nucleus or in special cases (Section 4). While comparison of the inner velocity rise for NGC 3198 showed good agreement between the 21-cm and the optical velocities (van Albada et al. 1985; Hunter et al. 1986), the agreement was poor for Virgo spirals observed at low HI resolution (Guhathakurta et al. 1988; Rubin et al. 1989). For low surface brightness galaxies, there is still discussion over whether the slow velocity rise is an attribute of the galaxy or due the instrumentation and reduction procedures (Swatters 1999, 2001; de Blok et al 2001; Section 7.5).

2.3 CO Line

The rotational transition lines of carbon monoxide (CO) in the millimeter wave range [e.g., 115.27 GHz for $^{12}\text{CO}(J = 1 - 0)$ line, 230.5 GHz for $J = 2 - 1$] are

valuable in studying rotation kinematics of the inner disk and central regions of spiral galaxies, for extinction in the central dusty disks is negligible at CO wavelengths (Sofue 1996, 1997). Edge-on and high-inclination galaxies are particularly useful for rotation curve analysis in order to minimize the uncertainty arising from inclination corrections, for which extinction-free measurements are crucial, especially for central rotation curves.

Because the central few kpc of the disk are dominated by molecular gas (Young & Scoville 1992; Young et al. 1995; Kenny & Young 1988; Garcia-Burillo et al. 1993; Nakai et al. 1995; Nishiyama & Nakai 1998; Sakamoto 1999), the molecular fraction, the ratio of the molecular-gas mass density to that of total of molecular and HI masses, usually exceeds 90% (Sofue et al. 1995; Honma et al. 1995). CO lines are emitted from molecular clouds associated with star formation regions emitting the H α line. Hence, CO is a good alternative to H α and also to HI in the inner disk, while HI is often weak or absent in the central regions. The H α , CO, and HI rotation curves agree well with each other in the intermediate region disks of spiral galaxies (Sofue 1996; Sofue et al. 1999a, b). Small displacements between H α and CO rotation curves can arise in the inner regions from the extinction of the optical lines and the contamination of the continuum star light from central bulges.

Decades ago, single dish observations in the mm wave range had angular resolutions limited from several to tens of arc seconds due to the aperture diffraction limit. Recently, however, interferometric observations have achieved sub- or one-arcsec resolution (Sargent and Welch 1993; Scoville et al. 1993; Schinnerer et al. 2000; Sofue et al. 2000), comparable to, or sometimes higher than, the current optical measurements (Fig. 1). Another advantage of CO spectroscopy is its high velocity resolution of one to several km s⁻¹.

2.4 Maser Lines

Radial velocity observations of maser lines, such as SiO, OH and H₂O lines, from circum-stellar shells and gas clouds allow us to measure the kinematics of stellar components in the disk and bulge of our Galaxy (Lindqvist et al. 1992a, b; Izumiura 1995, 1999; Deguchi et al. 2000). VLBI astrometry of SiO maser stars' proper motion and parallax as well as radial velocities will reveal more unambiguous rotation of the Galaxy in the future. VLBI measurements of water masers from nuclei of galaxies reveal circumnuclear rotation on scales of 0.1 pc around massive central black holes, as was successfully observed for NGC 4258 (Miyoshi et al. 1995; see Section 4.4).

2.5 Planetary Nebulae, Fabry-Perot, and Integral Field Spectrometers

Planetary nebulae (PN) are valuable tracers of the velocity fields of early type and complex galaxies, at large nuclear distances where the optical light is faint or absent (Jacoby et al. 1990; Arnaboldi 1998; Gerssen 2000), and for galaxies in clusters (Cen A, Hui et al. 1995; Fornax A, Arnaboldi et al. 1998). The

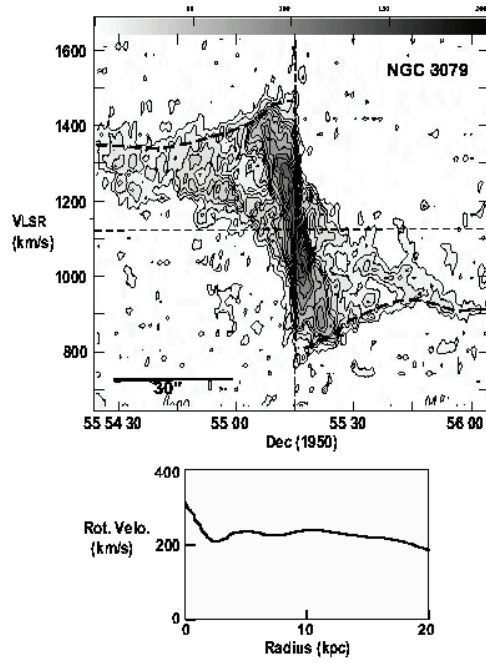


Figure 1: Position-velocity diagram along the major axis of the edge-on galaxy NGC 3079 in the CO ($J = 1 - 0$) line emission at a resolution of $1''.5$ observed with the 7-element interferometer consisted of the 6-element mm-wave Array and the 45-m telescope at Nobeyama (Sofue et al. 2000). The lower panel shows a composite rotation curve produced by combining the CO result and HI data (Irwin and Seaquist 1991) for the outer regions.

simultaneous analysis of absorption line velocities for inner regions and hundreds of PN in the outer regions can constrain the viewing geometry as no single tracer can, and thus reveal valuable details of the kinematics and the mass distribution (Rix et al. 1997; Arnaboldi et al. 1998).

Fabry-Perot spectrometers are routinely used to derive the H α velocity fields of spirals of special interest (Vaughan 1989; Vogel et al. 1993; Regan and Vogel 1994; Weiner & Williams 1996). Like Integral Field Spectrometry (Krabbe et al. 1997), these techniques will acquire more adherents as the instrument use and the reduction techniques become routine.

3 MEASURING ROTATION VELOCITIES

Although the mathematics of rotating disks is well established (e.g., Plummer 1911, Mestel, 1963, Toomre 1982, Binney & Tremaine 1987, Binney & Merrifield, 1998) the analysis of the observational data has continued to evolve as the quality of the data has improved. Both emission lines and absorption lines at a point on a spectrum are an integral along the line of sight through the galaxy. Only recently has the quality of the observational material permitted the deconvolution of various components. We describe a few procedures below.

3.1 Intensity-Weighted-Velocity Method

A rotation curve of a galaxy is defined as the trace of velocities on a position-velocity (PV) diagram along the major axis, corrected for the angle between the line-of-sight and the galaxy disk. A widely used method is to trace intensity-weighted velocities (Warner et al. 1973), which are defined by

$$V_{\text{int}} = \int I(v)v dv / \int I(v)dv, \quad (1)$$

where $I(v)$ is the intensity profile at a given radius as a function of the radial velocity. Rotation velocity is then given by

$$V_{\text{rot}} = (V_{\text{int}} - V_{\text{sys}})/\sin i, \quad (2)$$

where i is the inclination angle and V_{sys} is the systemic velocity of the galaxy.

3.2 Centroid-Velocity and Peak-Intensity-Velocity Methods

In outer galactic disks, where line profiles can be assumed to be symmetric about the peak-intensity value, the intensity-weighted velocity can be approximated by a centroid velocity of half-maximum values of a line profile (Rubin et al. 1980, 1982, 1985), or alternatively by a velocity at which the intensity attains its maximum, the peak-intensity velocity (Mathewson et al. 1992, 1996). Both methods have been adopted in deriving emission line rotation curves. Tests

indicate that centroid measures of weak emission lines show less scatter (Rubin, unpublished).

However, for inner regions, where the line profiles are not simple, but are superposition of outer and inner disk components, these two methods often under-estimate the true rotation velocity. The same situation occurs for edge-on galaxies, where line profiles are the superposition of profiles arising from all radial distances sampled along the line-of-sight. In these circumstances, the envelope-tracing method described below gives more reliable rotation curves.

3.3 Envelope-Tracing Method

This method makes use of the terminal velocity in a PV diagram along the major axis. The rotation velocity is derived by using the terminal velocity V_t :

$$V_{\text{rot}} = (V_t - V_{\text{sys}})/\sin i - (\sigma_{\text{obs}}^2 + \sigma_{\text{ISM}}^2)^{1/2}, \quad (3)$$

where σ_{ISM} and σ_{obs} are the velocity dispersion of the interstellar gas and the velocity resolution of observations, respectively. The interstellar velocity dispersion is of the order of $\sigma_{\text{ISM}} \sim 7$ to 10 km s^{-1} , while σ_{obs} depends on instruments.

Here, the terminal velocity is defined by a velocity at which the intensity becomes equal to

$$I_t = [(\eta I_{\text{max}})^2 + I_{\text{lc}}^2]^{1/2} \quad (4)$$

on observed PV diagrams, where I_{max} and I_{lc} are the maximum intensity and intensity corresponding to the lowest contour level, respectively, and η is usually taken to be 0.2 to 0.5. For $\eta = 0.2$, this equation defines a 20% level of the intensity profile at a fixed position, $I_t \simeq 0.2 \times I_{\text{max}}$, if the signal-to-noise ratio is sufficiently high. If the intensity is weak, the equation gives $I_t \simeq I_{\text{lc}}$ which approximately defines the loci along the lowest contour level (usually $\sim 3 \times$ rms noise).

For nearly face-on galaxies observed at sufficiently high angular resolution, these three methods give an almost identical rotation curve. However, both finite beam width and disk thickness along the line of sight cause confusion of gas with smaller velocities than the terminal velocity, which often results in a lower rotation velocity in the former two methods.

The envelope-tracing method is ill-defined when applied to the innermost part of a PV diagram, for the two sides of the nucleus have a discontinuity at the nucleus due principally to the instrumental resolution, which is large with respect to the velocity gradients. In practice, this discontinuity is avoided by stopping the tracing at a radius corresponding to the telescope resolution, and then approximating the rotation curve by a straight line crossing the nucleus at zero velocity. The ‘‘solid body’’ rotation implied by this procedure is probably a poor approximation to the true motions near the nucleus (Section 4.3).

3.4 Iteration Method

Takamiya and Sofue (private communication) have developed an iterative method to derive a rotation curve. This extremely reliable method comprises the follow-

ing procedure. An initial rotation curve, RC0, is adopted from a PV diagram (PV0), obtained by any method as above (e.g. a peak-intensity method). Using this rotation curve and an observed radial distribution of intensity (emissivity) of the line used in the analysis, a PV diagram, PV1, is constructed. The difference between this calculated PV diagram and the original PV0, e.g. the difference between peak-intensity velocities, is used to correct the initial rotation curve to obtain a corrected rotation curve, RC1. This RC is used to calculate another PV diagram PV2 using the observed intensity distribution, and to obtain the next iterated rotation curve, RC2 by correcting for the difference between PV2 and PV0. This iteration is repeated until PV_i and PV0 becomes identical, such that the summation of root mean square of the differences between PV_i and PV0 becomes minimum and stable. RC_i is adopted as the most reliable rotation curve.

3.5 Absorption Line Velocities

For several decades, the Fourier quotient technique (Simkin 1974, Sargent et al. 1977) or the correlation technique (Bender 1990, Franx & Illingworth 1988) were methods of choice for determining rotation velocities within early-type galaxies. Both procedures assume that the stellar absorption lines formed by the integration along the line of sight through the galaxy can be fit by a Gaussian profile. However, recent instrumental improvements confirm that even disk galaxies consist of multi-component kinematic structures, so more sophisticated methods of analysis are required to reveal velocity details of the separate stellar components.

Various methods have been devised to account for the non-Gaussian form of the line-of-sight velocity distribution. Line profiles can be expanded into a truncated Gauss-Hermite series (van der Marel & Franx 1993) which measure the asymmetric deviations (h_3) and the symmetric deviations (h_4) from Gaussian. Alternatively, one can use the unresolved Gaussian decomposition method (Kuijken and Merrifield 1993). Other procedures to determine line profiles and their higher order moments (e.g. Bender 1990, Rix & White 1992, Gerhard 1993) are in general agreement (Fisher 1997); differences arise from signal-to-noise, resolution, and template mismatch. Such procedures will define the future state-of-the-art.

3.6 Dependence on Observational Methods

Disk galaxies are a complex combination of various structural components. Observations from emission lines and absorption lines in the optical, mm, and radio regions may not sample identical regions along the same line-of-sight. Instruments sample at different sensitivities with different wavelength and spatial resolutions. Results are a function of the techniques of observations and reductions. A simple “rotation curve” is an approximation as a function of radius to the full velocity field of a disk galaxy. As such, it can be obtained only by neglecting small scale velocity variations, and by averaging and smoothing

rotation velocities from both sides of the galactic center. Because it is a simple, albeit approximate, description of a spiral velocity field, it is likely to be valuable even as more complex descriptions become available for many galaxies.

4 CENTRAL ROTATION CURVES

Centers of galaxies are still mysterious places. For galaxies as close as the Virgo cluster, $0.1''$ subtends about 8pc. Only in a few special cases can the stellar or gas kinematics be inferred on such scales: for very few galaxies can we sample velocity fields on scales of tens of parsecs. Generally, when astronomers discuss circumnuclear rotation curves, they refer to velocities measured from spectra where a single resolution element encompasses a large fraction of the radius on which the velocities vary. “High accuracy” and “high resolution” mean high with respect the present state-of-the-art.

4.1 High Resolution and Dynamic Range

A simulation reveals the effects of the finite resolution on the observed PV diagram, for a galaxy with assumed gas and mass distributions (Sofue 1999a). Fig. 2 shows an assumed rotation curve for a galaxy containing a central compact core, bulge, disk and massive halo, each expressed by a Plummer potential. In the observed PV diagram, however, the central steep rise and the peaks due to the core and bulge are hardly recognized. Central rotation curves derived from observed PV diagrams generally give *lower limits* to the rotation velocities. In fact, this conclusion holds for virtually all procedures which do not adequately account for the finite observed resolution.

CCD spectroscopy has made it possible to derive optical rotation curves of centers of galaxies, due to high dynamic range and precise subtraction of bulge continuum light (Rubin & Graham 1987; Woods et al. 1990; Rubin et al. 1997; Sofue et al. 1998, 1999a; Bertola et al. 1998). However, optical spectroscopy often encounters additional difficulty arising from extinction due to dusty nuclear disks as well as confusion with absorption features from Balmer wings of A-type stars. These problems are lessened at the wavelength of CO lines because of the negligible extinction, the high molecular gas content, and the high spatial and velocity resolution. At present, the combination of optical and CO-line spectroscopy produces rotation curves of high accuracy, reliable for the entire regions of galaxies including the central regions (Sofue 1996, 1997, Sofue et al. 1997, 1998, 1999).

In a few special cases, nuclear disks have been studied with other techniques. For several bright radio cores, HI absorption features have revealed high-velocity central disks (Ables et al. 1987; Irwin & Seaquist 1991). Rapidly rotating nuclear disks studied from their water maser emission and very high resolution observations are discussed in Section 4.4.

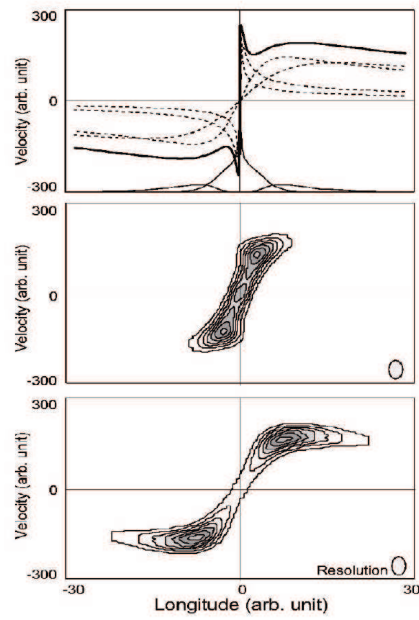


Figure 2: Simulation of the effect of beam-smearing on a position-velocity diagram. The top panel shows an assumed 'true' rotation curve comprising a central core, bulge, disk and a halo. Assumed molecular and HI gas distributions are indicated by the thin lines. The middle panel is an 'observed' PV diagram in CO, and the bottom in HI. Both the resolution and sensitivity are crucial to detect central high velocities and steep rise.

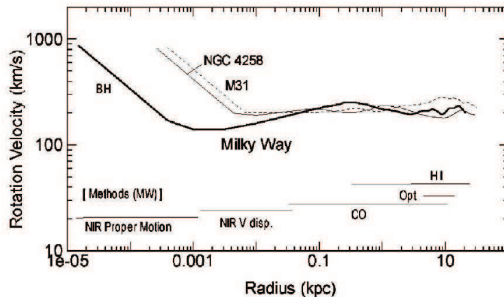


Figure 3: Logarithmic rotation curves of the Milky Way (thick line), NGC 4258 (thin line) and M31 (dashed line). Innermost rotation velocities are Keplerian velocities calculated for massive black holes. Observational methods for the Milky Way are shown by horizontal lines.

4.2 The Milky Way Center

By its proximity, our Galaxy provides a unique opportunity to derive a high resolution central rotation curve (Gilmore et al. 1990). Proper-motion studies in the near infrared show that the velocity dispersion of stars within the central 1 pc increases toward the center, indicating the existence of a massive black hole of mass $3 \times 10^6 M_{\odot}$ (Genzel et al. 1997, 2000; Ghez et al. 1998).

The rotation curve varies slightly depending upon the tracer. A rotation curve formed from high resolution CO and HI-line spectroscopy (Burton & Gordon 1978; Clemens 1985; Combes 1992), shows a very steep rise in the central hundred pc region, attaining a peak velocity of 250 km s^{-1} at $R \sim 300 \text{ pc}$. It then decreases to a minimum at $R \sim 3 \text{ kpc}$ of about 200 km s^{-1} , followed by a gentle maximum at 6 kpc and a flat part beyond the solar circle. Rotation velocities due to the black hole are combined with the outer velocities in Fig. 3: the curve is presented both in linear and logarithmic plots. Of course, the rotation velocity does not decline to zero at the nucleus, but increases inward, following a Keplerian law.

Radial velocities of OH and SiO maser lines from IR stars in the Galactic Center region are used to derive the velocity dispersion and the mass within the observed radius, as well as the mean rotation, which seems to take part in the Galactic rotation (Lindqvist et al. 1992a, b; Sjouwerman et al. 1998). SiO masers from IRAS sources in the central bulge have been used to study the kinematics, and the mean rotation of the bulge was found to be in solid body rotation of the order of 100 km s^{-1} (Izumiura et al. 1995; Deguchi et al. 2000). SiO masers in the disk region have been also used to study the structure and kinematics of a possible bar structure and non-circular streaming motion superposed on the disk and bulge components (Izumiura et al. 1999).

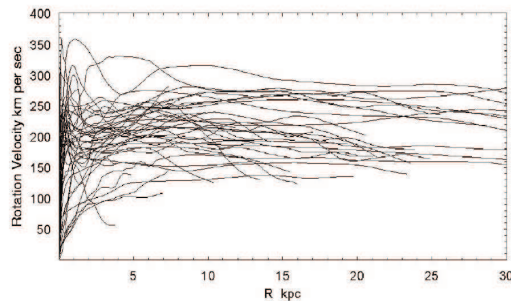


Figure 4: Rotation curves of spiral galaxies obtained by combining CO data for the central regions, optical for disks, and HI for outer disk and halo (Sofue et al. 1999).

4.3 Rapidly Rotating Central Components and Massive Cores

Central rotation curves have been produced for a number of galaxies by a systematic compilation of PV diagrams in the CO and H α lines (Sofue 1996; Sofue et al. 1997, 1998, 1999). Fig. 4 shows rotation curves obtained for nearby galaxies at high spatial and velocity resolution. For massive spiral galaxies, high nuclear velocities may be a universal property, but detected only with highest resolution observations. Even a decade ago, it was observed (Rubin & Graham 1987) that innermost velocities for some galaxies start from an already high velocity at the nucleus. But high central density may not be a characteristic only of massive galaxies. The nearby M33 ($1''=3\text{pc}$), a galaxy with a minimal “bulge”, exhibits velocities over the inner $\pm 200\text{pc}$ which are flat at about $V=100\text{ km s}^{-1}$ (Rubin 1987), and do not decrease to zero at the origin. Here too, the contribution from the falling density of a peaked central mass exceeds the density contribution from the disk.

Bertola et al. (1998) have emphasized that the high-velocity nuclear peaks observed in some spiral galaxies match the simulated PV diagrams for Keplerian rotation due to a massive ($\sim 10^9 M_{\odot}$) black hole, at equivalent resolution. Even more dramatic, the analysis of Maciejewski & Binney (2000) show that when a galaxy with an arbitrarily large central velocity gradient is observed with a slit wider than the instrumental point spread function, artifacts are generated in the spectra. Such artifacts can erroneously be interpreted as discrete kinematic components, and may account for some of the features observed in the spectra of Virgo galaxies (Rubin et al. 1999).

Evidence confirms that the steep nuclear rise observed in massive galaxies is real, and not due to a particular view of non-circular motions. The probability of looking at a bar side-on is larger than that of viewing one end-on. Hence there is a larger probability for apparently slower rotation than circular velocity. For these massive galaxies, the mass density increases toward the nucleus more

rapidly than expected from an exponential or de Vaucouleurs law. The widely adopted custom of drawing a rotation curve by linking positive and negative velocities from the opposite sides across the nucleus along the major axis is incorrect, at least for these massive galaxies.

4.4 Massive Black Holes and Circum-nuclear Rotation

For many spirals, the innermost region exhibits rapid rotation velocities (Carter & Jenkins 1993; van der Marel et al. 1994; Miyoshi et al. 1995; Kormendy & Richstone 1995; Richstone, et al. 1998, Bertola et al. 1998; Ferrarese 1999; Kormendy & Westpfahl 1989; Kormendy 2001). These high velocities offer evidence for massive nuclear black holes. Consequently, orbital velocities in the center decrease rapidly from a velocity close to the speed of light. Detecting these high central velocities will require both enormously high spatial and velocity resolution and is a program for the future.

At present, spectroscopic sub arcsecond seeing is limited to the Space Telescope Imaging Spectrographs (STIS) and a few ground based telescopes, except in special cases. STIS is now engaged in a major study of a sample of 54 Sb-Sc spirals, $V \leq 2000 \text{ km s}^{-1}$ to obtain spectra at $H\alpha$, within a few arcsec of the nucleus (Axon, unpublished). The aim is to measure black hole masses, or significant upper limits.

In one very special nearby galaxy, NGC 4258, water masers at 22 GHz are observed from a disk of radius 0.1 pc in Keplerian rotation about a mass of $3.9 \times 10^7 M_{\odot}$ (Nakai et al. 1993; Watson & Wallim 1994; Miyoshi et al. 1995; Herrnstein et al. 1999). The maximum rotation velocity is 900 km s^{-1} ; the rotation period is 800 years. VLBI observations of the water maser line have revealed a rapidly rotating nuclear torus of sub parsec scales in several nearby active galactic nuclei (NGC 3079: Haschick et al. 1990; Trotter et al. 1998; Sawada-Satoh et al. 2000; NGC 1068: Greenhill et al. 1996; NGC 4945: Greenhill et al. 1997).

4.5 Activity and Rotation Curves

One might ask whether the existence of massive objects in the nuclei, as suggested from the high central velocities, is correlated with nuclear activity. High-accuracy central rotation curves for starburst galaxies (NGC 253, NGC 1808, NGC 3034), Seyferts (NGC 1068, NGC 1097), LINERs (NGC 3521, NGC 4569, NGC 7331), and galaxies with nuclear jets (NGC 3079) (Sofue et al. 1999a; Brinks et al. 1997) show, however, no particular peculiarity. Even such a very active galaxy like NGC 5128 (Cen A) shows a rotation curve much like a normal galaxy (van Gorkom et al. 1990). The radio lobe galaxy NGC 3079 has both strong nuclear activity and usual rotation properties, but with very high central velocities (Sofue & Irwin 1992; Irwin & Sofue 1992; Sofue et al. 1999a). While these galaxies all show a very steep central velocity rise, such steep rise is generally observed for massive galaxies without pronounced central activity. Because the global rotation and mass distribution in active spirals are generally normal,

it is likely that nuclear activity is triggered by local and temporal causes around central massive cores and/or black holes.

4.6 Resonance Rings

The ring resonance in rotating disks will affect the kinematics and rotation of gas and stars in a galaxy disk. Rotation curves for several ring galaxies (Buta et al. 1995, 1999) exhibit normal rotation properties, showing a steep nuclear rise, high-velocity peak near the resonance ring, and flat velocities in the disk and halo. Simulations of rotation properties for a bar resonance mimic well the observed variations of rotation velocities, which is of the order of $\pm 20 - 30 \text{ km s}^{-1}$ (Salo et al. 1999).

4.7 Nuclear Warp

A major interest in current interferometer observations of the CO line emissions from nuclear regions is the detailed orientation of the nuclear molecular disk (NMD) and circum-nuclear torus. A NMD is produced by accretion of disk gas due to an angular momentum transfer to the massive disk by galactic shock waves, either in spiral arms or bars, whereas off-axis angular momentum such as associated with warping is invariant. If the accreting disk has a warp, as is often the case and is particularly prominent in mergers and interacting galaxies, the displacement of angular momentum of accreting disk from the original rotation axis is amplified. Hence, NMDs often exhibit significant warp from the main disk. Interferometric CO observations exhibit that NGC 3079's NMD is warped from the main disk by 20 degrees which contains a higher-density molecular core inclined from both the NMD and main disk (Sofue et al. 2000); NGC 1068 shows an warped nuclear disk surrounding a nuclear torus whose axis is quite different from that of the main disk and nuclear disk (Kaneko et al. 1997; Schinnerer et al. 2000). A nuclear warp produces uncertain inclination corrections in the rotation velocities. These can be minimized by observing edge-on galaxies.

4.8 Nuclear Counterrotation

An extreme case of a nuclear warp is counterrotation. Rotating nuclear disks of cold gas have been discovered in more than 100 galaxies, types E through Sc (Bertola & Galletta 1978; Galletta 1987, 1996; Bertola et al. 1990; Bertola et al. 1992; Rubin 1994b; Garcia-Burillo et al. 1998); counterrotation is not especially rare. Simulations of disk interactions and mergers which include gas and stellar particles (Hernquist & Barnes 1991; Barnes & Hernquist 1992) reveal that a kinematically distinct nuclear gas disk can form; it may be counterrotating. Simulation of galactic-shock accretion of nuclear gas disk in an oval potential, such as a nuclear bar, produces highly eccentric streaming motion toward the nucleus, some portion being counterrotating (Wada et al. 1999). Kinematically decoupled *stellar* nuclear disks are also observed in early type galaxies (Jedrzejewski & Schechter 1989; Franx et al. 1991). Counter rotating nuclear disks

can result from merger, mass exchange and/or inflow of intergalactic clouds. In addition to forming the central disk, an inflow of counterrotating gas would also be likely to promote nuclear activity.

4.9 Non-circular Motion in Nuclear Molecular Bar

Oval potential such as due to a bar produces galactic shocks of interstellar gas, and the shocked gas streams along the bar in non-circular orbits (Sorensen et al. 1976; Noguchi 1988; Wada & Habe 1992, 1995; Shlosman 1990). The velocity of streaming motion during its out-of-shock passage is higher than the circular velocity, while the velocity during its shock passage is much slower than circular velocity, close to the pattern speed of the bar in rigid-body rotation. The molecular gas is strongly condensed in the galactic shock, and stays there for a large fraction of its orbiting period. Hence, CO line velocities manifest the velocity of shocked gas, and therefore, observed CO velocities are close to those of gas in rigid-body motion with a bar, slower than the circular velocity. This results in underestimated rotation velocities. Geometrical effect that the probability of side-on view of a bar is greater than that of end-on view also causes underestimated rotation velocities.

Bar-driven non-circular motion of the order of 20 to 50 km s⁻¹ are observed in central molecular disks (Ishizuki et al. 1990; Handa et al. 1990; Sakamoto et al. 1999; Kenney et al. 1992; Kohno 1998; Kohno et al. 1999). The CO-line PV diagram in the Milky Way Center (Bally et al. 1985; Oka et al. 1998; Sofue 1995) shows that the majority (~ 95%) of gas is rotating in steep rigid-body features. A few percent exhibits non-circular 'forbidden' velocities, which could be due to non-circular motion in an oval potential (Binney et al. 1991), whereas a question remains why the majority of the gas is regularly rotating. Because the gas is shocked and intensity-weighted velocities are smaller than the circular velocity as discussed above, determination of mass distribution in barred galaxies from observed CO velocities is not straightforward, and will be a challenge for numerical simulations in the future.

5 DISK ROTATION CURVES

A disk rotation curve manifests the distribution of surface mass density in the disk, attaining a broad maximum at a radius of about twice the scale radius of the exponential disk. For massive Sb galaxies, the rotation maximum appears at a radius of 5 or 6 kpc, which is about twice the scale length of the disk. Beyond the maximum, the rotation curve is usually flat, merging with the flat portion due to the massive dark halo. Superposed on the smooth rotation curve are fluctuations of a few tens of km s⁻¹ due to spiral arms or velocity ripples. For barred spirals, the fluctuations are larger, of order 50 km s⁻¹, arising from non circular motions in the oval potential.

5.1 Statistical Properties of Rotation Curves

The overall similarity of shapes of rotation curves for spiral galaxies has led to a variety of attempts to categorize their forms, and to establish their statistical properties. Kyazumov (1984) cataloged rotation curve parameters for 116 normal S and Ir galaxies, and categorized the shapes. Rubin et al. (1985) formed families of Sa, Sb, and Sc synthetic rotation curves as a function of luminosity, from the galaxies they had observed. Casertano & van Gorkom (1991), using HI velocities, studied rotation curves as a function of luminosity.

Mathewson et al. (1992, 1996) used their massive set of $H\alpha$ rotation curves together with optical luminosity profiles for 2447 southern galaxies, to examine the Tully-Fisher (1977) relation. For a subset of 1100 optical and radio rotation curves, Persic et al. (1995, 1996) fit the curves by a formula, which is a function of total luminosity and radius, comprising both disk and halo components. Both the forms and amplitudes are functions of the luminosity, and the outer gradient of the RC is a decreasing function of luminosity. Their formula does not contain any free parameters, and they call it universal rotation curve. Courteau (1997) obtained optical long-slit rotation curves for 304 Sb-Sc northern UGC galaxies for Tully-Fisher applications, and fitted the curves empirically by a simple function for the purpose to calculate line widths. Roscoe (1999) has attempted to parameterize outer-disk rotation curves by an extremely simple power law of radius.

Universal rotation curves reveal the following characteristics. Most luminous galaxies show a slightly declining rotation curves in the outer part, following a broad maximum in the disk. Intermediate galaxies have nearly flat rotation from across the disk. Less luminous galaxies have monotonically increasing rotation velocities across the optical disk. While Persic et al. conclude that the dark-to-luminous mass ratio increases with decreasing luminosity, mass deconvolutions are far from unique.

A study of 30 spirals in the Ursa Major Cluster (Verheijen 1997) showed that 1/3 of the galaxies (chosen to have kinematically unperturbed gas disks) have velocity curves which do not conform to the universal curve shape. Like humans, rotation curves have their individualities, but they share many common characteristics. These common properties are meaningful in some situations: in other circumstances their use may be misleading. It is important to apply the common properties only in appropriate situations, e.g., for outer disk and halo beyond ~ 0.5 optical radii, corresponding to several kpc for Sb and Sc galaxies. Inner rotation curves have greater individuality (Sofue et al. 1999a).

5.2 Environmental Effects in Clusters

A variety of physical mechanisms can alter the internal kinematics of spirals in clusters, just as these mechanism have altered the morphology of galaxies in clusters (Dressler 1984; Cayatte et al. 1990). Gas stripping, star stripping, galaxy-galaxy encounters, and interaction with the general tidal field are all likely to occur. Early studies of optical rotation curves for galaxies in clusters

(Burstein et al. 1986; Rubin et al. 1988; Whitmore et al. 1988, 1989) detected a correlation between outer rotation-velocity gradients and distances of galaxies from the cluster center. Inner cluster galaxies show shallower rotation curves than outer cluster galaxies, for distances 0.25 to 5 Mpc from cluster centers. These authors suggest that the outer galaxy mass is truncated in the cluster environment. Later studies have failed to confirm this result (Amram et al. 1992, 1993, 1996; Sperandio et al. 1995).

A study of rotation curves for 81 galaxies in Virgo (Rubin et al. 1999, Rubin & Hathiwanger 2001) shows that about half (43) have rotation curves identified as disturbed. Abnormalities include asymmetrical rotation velocities on the two sides of the major axis, falling outer rotation curves, inner velocity peculiarities, including velocities hovering near zero at small radii, and dips in mid-disk rotation velocities. Kinematic disturbance is not correlated with morphology, luminosity, Hubble type, inclination, maximum velocity, magnitude, or local galaxy density.

Virgo spirals with disturbed kinematics have a Gaussian distribution of systemic velocities which matches that of the cluster ellipticals; spirals with regular rotation show a flat distribution. Both ellipticals and kinematically disturbed spirals are apparently in the process of establishing an equilibrium population. H α emission extends farther in the disturbed spirals; the gravitational interactions have also enhanced star formation. The distribution on the sky and in systemic velocity suggests that kinematically disturbed galaxies are on elongated orbits which carry them into the cluster core, where galaxy-cluster and galaxy-galaxy interactions are more common and stronger. Self-consistent N-body models that explore the first pass of two gravitationally interacting disk galaxies (Barton et al. 1999) produce rotation curves with mid-region velocity dips matching those observed. Models of disk galaxies falling for the first time into the cluster mean field (Valluri 1993) show $m=1$ (warp) and $m=2$ (bar and spiral arms) perturbations.

5.3 Lopsided Position-Velocity Diagrams

There is increased interest in galaxies with kinematically lopsided HI profiles (Baldwin 1980; Sancisi 2001), which can arise from a large-scale asymmetry of HI gas distribution in the spiral disk. Of 1700 HI profiles, at least 50% show asymmetries (Richter & Sancisi 1994); recent work (Haynes et al. 1998) confirms this fraction. Because HI profiles result from an integration of the velocity and the HI distribution, *resolved* HI velocity fields offer more direct information on kinematic lopsidedness. From resolved HI velocity fields, Swaters et al. (1999) also estimate the disturbed fraction to be at least 50%.

As noted above, about 50% of Virgo spirals show optical major axis velocity disturbances; how this figure translates into lopsided HI profiles is presently unclear. The field spirals studied earlier by Rubin et al. (1985), chosen to be isolated and without obvious morphological peculiarities, have rotation curves which are *very* normal (74%; Rubin et al. 1999). Yet the sample of optical rotation curves for galaxies in the Hickson groups (Rubin et al. 1991) shows

noticeably lopsided rotation curves for $\geq 50\%$. Further studies are needed to establish the frequency of lopsidedness as a function of luminosity, morphology, HI content, resolution, sensitivity, extent of the observations, and environment.

5.4 Counterrotating Disks and Other Kinematic Curiosities

Only a handful of galaxies are presently known to have counterrotating components over a large fraction of their disks (Rubin 1994b). The disk of E7/S0 NGC 4550, (Rubin et al. 1992; Kenney & Faundez 2000) contains two hospital stellar populations, one orbiting programmed, one retrograde. This discovery prompted modification of computer programs which fit only a single Gaussian to integrated absorption lines in galaxy spectra (Rix et al. 1992). In NGC 7217 (Sab), 30% of the disk stars orbit retrograde (Merrifield & Kuijen 1994). The bulge in NGC 7331 (Sbc) may (Prada et al. 1996) or may not (Mediavilla et al. 1998) counterrotate with respect to the disk. Stars in NGC 4826 (Sab; the Black Eye or Sleeping Beauty) orbit with a single sense. Gas extending from the nucleus through the broad dusty lane rotates prograde, but reverses its sense of rotation immediately beyond; radial infall motions are present where the galaxy velocities reverse (Rubin et al. 1965; Braun et al. 1994; Rubin 1994a; Walterbos et al. 1994; Rix et al. 1995; Sil'chenko 1996).

However, galaxies with extended counterrotating disks are not common. A peculiar case is the early type spiral NGC 3593, which exhibits two cold counterrotating disks (Bertola et al. 1996). Of 28 S0 galaxies examined by Kuijken (1996), none have counterrotating components accounting for more than 5% of the disk light (see also Kannappan & Fabricant 2000). Formation mechanisms for counterrotating disks can be devised (Thaker & Ryden 1998), although cases of failure are reported only anecdotally (Spergel, private communication). While such galaxies are generally assumed to be remnants of mergers, models show that generally the disk will heat up and/or be destroyed in a merger.

In an effort to circumvent the problem of disk destruction in a merger, Evans & Collett (1994) devised a mechanism for producing equal numbers of prograde and retrograde stellar disk orbits, by scattering stars off a bar in a galaxy whose potential slowly changes from triaxial to more axisymmetric. In an even more dramatic solution by Tremaine & Yu (2000; see also Heisler et al. 1982; van Albada et al. 1982) polar rings and/or counterrotating stellar disks can arise in a disk galaxy with a triaxial halo. As the pattern speed of the initially retrograde halo changes to prograde due to infalling dark matter, orbits of disk stars caught at the Binney resonance can evolve from prograde to retrograde disk orbits. If, instead, the halo rotation decays only to zero, stars with small inclinations are levitated (Sridhar & Touma 1996) into polar orbits. This model predicts that stellar orbits in a polar ring will be divided equally into two! counterrotating streams, making this a perfect observing program for a very large telescope.

As spectral observations obtain higher resolution and sensitivity, emission from weaker components is measured. HI observations of NGC 2403 reveal a normal rotation, plus more slowly rotating HI extensions in a PV diagram, the

“beard”, which can be due to an infall of gas from an extended HI halo with slower rotation, perhaps from a galactic fountain flow (Schaap et al. 2000). Higher sensitivity VLA observations of NGC 2403 have detected HI in the forbidden velocity quadrants, which can be due to a radial inflow (Fraternali et al. 2000). Improved instrumentation permits detection of weaker features, so we glimpse the kinematic complexities which exist in minor populations of a single galaxy.

Edge-on and face-on spirals are fine laboratories for studying vertical kinematics. In the edge on NGC 891, HI extends about 5 kpc above the plane, where it rotates at about 25 km s^{-1} , more slowly than the disk (Swaters et al. 1997). Slower rotation is also observed in the CO halo in the edge on dwarf M82 (Sofue et al. 1992). Face on galaxies like M101 and NGC 628 show often extended HI disk showing different kinematical properties from the disk (Kamphuis et al. 1991; Kamphuis & Brigg 1992).

5.5 Rotation of High Redshift Galaxies

Only recently have rotation curves been obtained for distant galaxies, using HST and large-aperture ground-based telescopes with sub-arc second seeing. We directly observe galaxy evolution by studying galaxies closer to their era of formation. Rotation velocities for moderately distant spirals, $z \approx 0.2$ to 0.4 , (Bershady 1997, et al. 1999, Simard & Prichet 1998, Kelson et al. 2000a) have already been surpassed with Keck velocities reaching $z \approx 1$ (Vogt et al. 1993, 1996, 1997; Koo 1999), for galaxies whose diameters subtend only a few seconds of arc. The rotation properties are similar to those of nearby galaxies, with peak velocities between 100 to 200 km s^{-1} , and flat outer disk velocities.

Regularly rotating spiral disks existed at $z \approx 1$, when the universe was less than half of its present age. The Keck rotation velocities define a TF relation (i.e., the correlation of rotation velocity with blue magnitude) which matches to within ≤ 0.5 magnitudes that for nearby spirals. Spiral galaxy evolution, over the last half of the age of the universe, has not dramatically altered the TF correlation.

5.6 Rotation Velocity as a Fundamental Parameter of Galaxy Dynamics and Evolution

The maximum rotation velocity, reached at a few galactic-disk scale radii for average and larger sized spiral galaxies, is equivalent to one-half the velocity width of an integrated 21 cm velocity profile. The Tully-Fisher relation (1977; Aaronson et al. 1980; Aaronson & Mould 1986), the correlation between total velocity width and spiral absolute magnitude, represents an oblique projection of the fundamental plane of spiral galaxies, which defines a three-dimensional relation among the radius, rotation velocity, and luminosity (absolute magnitude) (Steinmetz & Navarro 1999; Koda et al. 2000a,b). The shape of a disk rotation curve manifests the mass distribution in the exponential-disk, which is the

result of dissipative process of viscous accreting gas through the proto-galactic disk evolution (Lin & Pringle 1987).

As such, it emphasizes the essential role that rotation curves play in determining the principal galactic structures, and in our understanding of the formation of disk galaxies (e.g. Mo et al. 1998). For elliptical galaxies, the three parameter (half-light radius, surface brightness, and central velocity dispersion) fundamental plane relation (Bender et al. 1992; Burstein et al. 1997) is a tool for studying elliptical galaxy evolution, analogous to the spiral TF relation. Keck spectra and HST images of 53 galaxies in cluster CL1358+62 ($z=0.33$) define a fundamental plane similar to that of nearby ellipticals (Kelson et al. 2000b). Ellipticals at $z=0.33$ are structurally mature; data for more distant ellipticals should be available within several years.

6 HALO ROTATION CURVES AND DARK MATTER: A Brief Mention

The difference between the matter distribution implied by the luminosity, and the distribution of mass implied by the rotation velocities, offers strong evidence that spiral galaxies are embedded in extended halos of dark matter. The physics of dark matter has been and will be one of the major issues to be studied by elementary particle physicists and astronomers.

6.1 Flat Rotation Curve in the Halo

When Rubin & Ford (1970) published the rotation curve of M31, formed from velocities of 67 HII regions, they noted that the mass continued to rise out to the last measured region, 24 kpc. They concluded “extrapolation beyond that distance is clearly a matter of taste”. By 1978, Rubin et al. (1978) had learned that “rotation curves of high luminosity spiral galaxies are flat, at nuclear distances as great as 50 kpc” ($H_0 = 50 \text{ km s}^{-1} \text{ Mpc}^{-1}$). Flat HI rotation curves were first noticed (Roberts & Rots 1973) using a single dish telescope. However, it would be a few years before the observers and the theorists (Ostriker & Peebles 1973; Ostriker et al. 1974, Einasto et al. 1974) recognized each others’ work, and collectively asserted that disk galaxies are immersed in extended dark matter halos.

Deeper and higher-resolution HI observations with synthesis telescopes reveal that for the majority of spiral galaxies, rotation curves remain flat beyond the optical disks (Bosma 1981a, b; Guhathakurta et al. 1988; van Albada et al. 1985; Begeman 1989). The Sc galaxy UGC 2885 has the largest known HI disk, with HI radius of 120 kpc for $H_0 = 50 \text{ km s}^{-1} \text{ Mpc}^{-1}$ (85 kpc for $H_0 = 70 \text{ km s}^{-1} \text{ Mpc}^{-1}$); the HI rotation curve is still flat (Roelfsema & Allen 1985).

The conclusion that a flat rotation curve is due to a massive dark halo surrounding a spiral disk requires that Newtonian gravitational theory holds over cosmological distances. Although proof of this assumption is lacking, most

astronomers and physicists prefer this explanation to the alternative, that Newtonian dynamics need modification for use over great distances. For readers interested in such alternatives, see Milgrom (1983), Sanders (1996), McGaugh & de Blok (1998), de Blok & McGaugh (1998), Begeman et al. (1991), Sanders (1996), Sanders & Verheijen (1998). Non gravitational acceleration of halo gas rotation would be also an alternative, such as due to magneto-hydrodynamical force (Nelson 1998).

6.2 Massive Dark Halo

One of the best indicators of dark matter is the difference between the galaxy mass predicted by the luminosity and the mass predicted by the velocities. This difference, which also produces a radial variation of the mass-to-luminosity ratio (M/L), is a clue to the distribution of visible and dark (invisible) mass (e.g., Bosma 1981a, b; Lequeux 1983; Kent 1986, 1987; Persic & Salucci 1988, 1990; Salucci & Frenk 1989; Forbes 1992; Persic et al. 1996; Héraudeau & Simien 1997; Takamiya & Sofue 2000). Unfortunately, there is not yet a model independent procedure for determining the fraction of mass contained in the bulge, disk, and dark halo, and mass deconvolutions are rarely unique. Most current investigations assume that the visible galaxy consists of a bulge and a disk, each of constant M/L . Kent (1986, 1991, 1992) has used the “maximum-disk method” to derive averaged M/L s in the individual components. Athanasoula et al. (1987) attempted to minimize the uncertainty between maximum and minimal disks by introducing constraints to allow for the existence of spiral structure. Discussions of maximum or non-maximum disk persist (Courteau and Rix 1999), even for our Galaxy (van der Kruit 2000).

Radial profiles of the surface-mass density (SMD) and surface luminosity can be used to calculate M/L directly. Forbes (1992) derived the radial variation in the ratio of the total mass to total luminosity involved within a radius, r , an ‘integrated M/L ’. Takamiya and Sofue (2000) determine the SMD directly from the rotation curves, which can be sandwiched by mass distributions calculated from rotation curves on both spherical and flat-disk assumptions by solving directly the formula presented by Binney and Tremaine (1987). A comparison of the SMD distributions with optical surface photometry shows that the radial distributions of the M/L ratio is highly variable within the optical disk and bulge, and increases rapidly beyond the disk, where the dark mass dominates.

Separation of halo mass from disk mass, whether dark or luminous, is an issue for more sophisticated observations and theoretical modeling. Weiner et al. (2000a, b) have used non-circular streaming motion to separate the two components using their theory that the streaming motion in a bar potential is sensitive to the halo mass.

6.3 The Extent of the Milky Way Halo

Interior to the Sun’s orbit, the mass of the Galaxy is $\approx 10^{11}M_{\odot}$. Although there is evidence that the halo rotation curve is declining beyond 17 kpc in a

Keplerian fashion (Honma & Sofue 1997a), the mass distribution beyond the HI disk, e.g. at > 22 kpc, is still controversial. Interior to the distance of the Large Magellanic Cloud, the Galaxy mass may grow to $6 \times 10^{11} M_{\odot}$ (Wilkinson & Evans 1999), which depends upon the assumed orbit of the Cloud. Interior to 200 kpc, the mass is at least $2 \times 10^{12} M_{\odot}$ (Peebles 1995), matching masses for a set of Milky Way-like galaxies with masses inferred statistically from the velocities of their satellite galaxies (Zaritsky 1992).

A Milky Way halo which extends at least 200 kpc is getting close to the half-way distance between the Galaxy and M31, 350 kpc. And if halos are as large as those suggested by the gravitational distortion of background galaxies seen in the vicinity of foreground galaxies (Fischer et al. 2000; Hoekstra 2000), then the halo of our Galaxy may brush the equivalently large halo of M31.

6.4 Declining Rotation Curves

Few spirals exhibit a true Keplerian decline in their rotation velocities. Among peculiar rotation curves, declining rotation curves are occasionally observed, confirming the conventional belief that the mass distribution is truncated at about 1 to 3 optical radii (3-5 scale lengths) (Casertano 1983; Casertano & van Gorkom 1991; Barteldrees & Dettman 1994). Yet some galaxies exhibit Keplerian rotation curves well beyond the critical truncation radius (Honma & Sofue 1997a, b). While truncation is an important issue for those who wish to weaken the notion of a conspiracy of luminous and dark matter (Casertano & van Gorkom 1991), the issue is far from resolved.

7 GALAXY TYPES AND ROTATION CHARACTERISTICS

There is a marked similarity of form, but not of amplitude, of disk and halo rotation curves for galaxies with different morphologies from Sa to Sc (Rubin et al. 1985). Thus the form of the gravitational potential in the disk and halo is not strongly dependent on the form of the optical luminosity distribution. Some moderate correlation is found between total luminosity and rotation velocity amplitude. Also, less luminous galaxies tend to show increasing outer rotation curve, while most massive galaxies have slightly declining rotation in the outmost part (Persic et al. 1996). On the other hand, form of central rotation curves depend on the total mass and galaxy types (Sofue et al. 1999): Massive galaxies of Sa and Sb types show a steeper rise and higher central velocities within a few hundred pc of the nucleus compared to less massive Sc galaxies and dwarfs. Dwarf galaxies generally show a gentle central rise.

7.1 Sa, Sb, Sc Galaxies

The maximum rotation velocities for Sa galaxies are higher than those of Sb and Sc galaxies with equivalent optical luminosities. Median values of V_{\max} decreases

from 300 to 220 to 175 km s⁻¹ for the Sa, Sb, and Sc types, respectively (Rubin et al. 1985).

Sb galaxies have rotation curves with slightly lower values of the maximum velocity than Sa (Rubin et al. 1982). The steep central rise at 100-200 pc is often associated with a velocity peak at radii $r \sim 100 - 300$ pc (Sofue et al. 1999a). The rotation velocity then declines to a minimum at $r \sim 1$ kpc, and is followed by a gradual rise to a broad maximum at $r \sim 2 - 7$ kpc, arising from the disk potential. The disk rotation curve has superposed amplitude fluctuations of tens of km s⁻¹ due to spiral arms or velocity ripples. The outermost parts are usually flat, due to the massive dark halo. Some Sb galaxies show a slight outer decline, often no larger than the inner undulations (Honma & Sofue 1997a, b).

The rotation curve of the Milky Way Galaxy, a typical Sb galaxy, is shown in Fig. 2 (Clemens 1985; Blitz 1979; Brand and Blitz 1993; Fich et al. 1989; Merrifield 1992; Honma and Sofue 1995). The rotation curve of Sb galaxies, including the Milky Way, can be described as having: (a) a high-density core, including the massive black hole, which causes a non-zero velocity very close to the center; (b) a steep rise within the central 100 pc; (c) a maximum at radius of a few hundred pc, followed by a decline to a minimum at 1 to 2 kpc; then, (d) a gradual rise from to the disk maximum at 6 kpc; and (e) a nearly flat outer rotation curve.

Sc galaxies have lower maximum velocities than Sa and Sb (Rubin et al. 1980; 1985), ranging from ≤ 100 to ~ 200 km s⁻¹. Massive Sc galaxies show a steep nuclear rise similar to Sb's. However, less-massive Sc galaxies have a more gentle rise. They also have a flat rotation to their outer edges. Low-surface brightness Sc galaxies have a gentle central rise with monotonically increasing rotation velocity toward the edge, similar to dwarf galaxies (Bosma et al. 1988).

7.2 Barred Galaxies

Large-scale rotation properties of SBb and SBc galaxies are generally similar to those of non-barred galaxies of Sb and Sc types. However, the study of their kinematics is more complicated than for non-barred spirals, because their gas tracers are less uniformly distributed (Bosma 1981a,1996), and their iso-velocity contours are skewed in the direction toward the bar (H α , Peterson et al. 1978; HI, Sancisi et al. 1979; stellar absorption lines, Kormendy 1983). CO-line mapping and spectroscopy reveal high concentration of molecular gas in shocked lanes along a bar superposed by significant non-circular motions (Handa et al. 1990; Sakamoto et al. 1999; Kuno et al. 2000). Thus, barred galaxies show velocity jumps from $\pm \sim 30 - 40$ km s⁻¹ to ≥ 100 km s⁻¹ on the leading edges of the bar, $R \sim 2 - 5$ kpc, whereas some barred galaxies show flat rotation (e.g., NGC 253: Sorai et al. 2000). Non-barred spirals can show velocity variation of about $\pm 10 - 20$ km s⁻¹, caused mainly by spiral arms. Compared with non-barred spirals, barred galaxies require a more complete velocity field to understand their kinematics. As discussed earlier, intensity-weighted velocities are underestimated compared to the circular velocities, which is particularly crucial for shock compressed molecular gas in the central regions (see Section

4.9).

This large velocity variation arises from the barred potential of several kpc length. Simulations of PV diagrams for edge-on barred galaxies show many tens of km s^{-1} fluctuations, superposed on the usual flat rotation curve (Athanasoula and Bureau 1999; Bureau and Athanassoula 1999; Weiner & Sellwood 1999). However, distinguishing the existence of a bar and quantifying it are not uniquely done from such limited edge-on information. For more quantitative results, two-dimensional velocity analyses are necessary (Wozniak & Pfenniger 1997). In these models, barred spirals contain up to 30% counterrotating stars; the orbits are almost circular and perpendicular to the bar. Pattern speeds for the bar have been determined from absorption line spectra (Buta et al. 1996; Gerssen 2000 and references therein).

Due to their kinematic complexity, barred galaxies have been observed considerably less than non-barred, even though they constitute a considerable fraction of all disk galaxies (Mulchaey & Regan 1997). However, high resolution optical observations, combined with HI and CO, have helped to stimulate the study of two-dimensional non-circular velocity fields (e.g. Wozniak & Pfenniger 1997, Hunter & Gottesman 1996; Buta et al. 1996). Gas streaming motions along the bar are an efficient way to transport gas to the nuclear regions (Sorensen et al. 1976; Schwartz 1981; Noguchi 1988; Wada & Habe 1992, 1995; Wada et al. 1998; Shlosman et al. 1990), and lead to enhanced star formation.

7.3 Low Surface Brightness Galaxies; Dwarf Galaxies

Until the last decade, observations of rotational kinematics were restricted to spirals with average or high surface brightness. Only within the past decade have low surface brightness (LSB) galaxies been found in great numbers (Schombert & Bothun 1988; Schombert et al. 1992); many are spirals. Their kinematics were first studied by de Blok et al. (1996) with HI, who found slowly rising curves which often continued rising to their last measured point. However, many of the galaxies are small in angular extent, so observations are subject to beam smearing. Recent optical rotation curves (Swaters 1999, 2001; Swaters et al. 2000; de Blok et al. 2001) reveal a steeper rise for some, but not all, of the galaxies studied previously at 21-cm. It is not now clear if LSB galaxies are as dominated by dark matter as they were previously thought to be; the mass models have considerable uncertainties.

Dwarf galaxies, galaxies of low mass, are often grouped with low surface brightness galaxies, either by design or by error. The two classes overlap in the low surface brightness/low mass region. However, some low surface brightness galaxies are large and massive; some dwarf galaxies have high surface brightness. Early observations showed dwarf galaxies to be slowly rotating, with rotation curves which rise monotonically to the last measured point (Tully et al. 1978; Carignan & Freeman 1985; Carignan & Puche 1990a,b; Carignan & Beaulieu 1989; Puche et al. 1990, 1991a, b; Lake et al. 1990; Broeils 1992). The dark matter domination of the mass of the dwarf galaxy NGC 3109 (Carignan 1985; Jobin & Carignan 1990) is confirmed by a reanalysis including $\text{H}\alpha$ Fabry-Perot

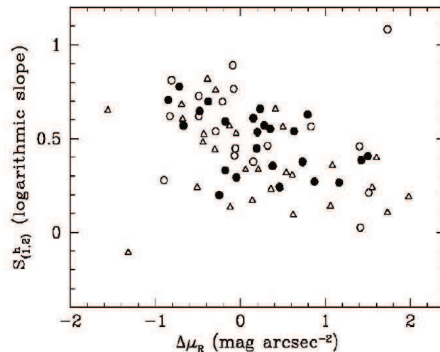


Figure 5: The logarithmic slope of rotation curves between one and two scale radii, plotted against the central concentration of light, $\Delta\mu_R = \mu_0 - \mu_c$, where μ_c is the observed central surface brightness and μ_0 the extrapolated surface brightness of the exponential disk. Galaxies with larger excess of central brightness have flatter rotation. Filled and open circles are dwarfs (high and low accuracy), and triangles are spirals. [Courtesy of R. Swaters (1999)]

data (Blais-Ouellette et al. 2000a, b). An exceptional case of a declining outer rotation curve has been found in the dwarf galaxy NGC 7793 (Carignan & Puche 1990a). $H\alpha$ velocity field observations of blue compact galaxies, with velocities less than 100 km s^{-1} , show that rotation curves rise monotonically to the edges of the galaxies (Östlin et al. 1999).

Swaters (1999) derived rotation curves from velocity fields obtained with the Westerbork Synthesis Radio Telescope for 60 late-type dwarf galaxies of low luminosity. By an interactive analysis, he obtained rotation curves which are corrected for a large part of the beam smearing. Most of the rotation curve shapes are similar to those of more luminous spirals; at the lowest luminosities, there is more variation in shape. Dwarfs with higher central light concentrations have more steeply rising rotation curves, and a similar dependence is found for disk rotation curves of spirals (Fig. 5). For dwarf galaxies dominated by dark matter, as for LSB (and also HSB) spirals, the contributions of the stellar and dark matter components to the total mass cannot be unambiguously derived. More high quality observations and less ambiguous mass deconvolutions, perhaps more physics, will be required to settle questions concerning the dark matter fraction as a function of mass and/or luminosity.

7.4 Large Magellanic Cloud

The LMC is a dwarf galaxy showing irregular optical morphology, with the enormous starforming region, 30 Dor, located significantly displaced from the optical bar and HI disk center. High-resolution HI kinematics of the Large

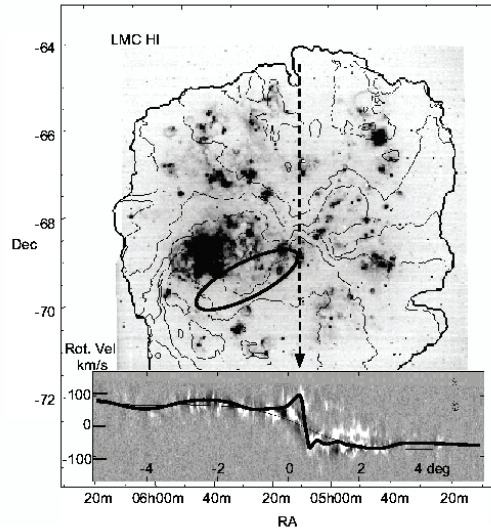


Figure 6: The HI velocity field of the LMC superposed on an $H\alpha$ image, and a position-velocity diagram across the kinematical major axis (Kim et al. 1998: Courtesy of S. Kim). The ellipse indicates the position of the optical bar. The thick line in the PV diagram traces the rotation curve, corrected for the inclination angle of 33° .

Magellanic Cloud, Kim et al. (1998; see Westerlund 1999 review) indicate, however, a regular rotation around the kinematical center, which is displaced 1.2 kpc from the center of the optical bar as well as from the center of starforming activity (Fig. 6). The rotation curve has a steep central rise, followed by a flat rotation with a gradual rise toward the edge. This implies that the LMC has a compact bulge (but not visible on photographs), an exponential disk, and a massive halo. This dynamical bulge is 1.2 kpc away from the center of the stellar bar, and is not associated with an optical counterpart. The “dark bulge” has a large fraction of dark matter, with an anomalously high mass-to-luminosity (M/L) ratio (Sofue 1999). In contrast, the stellar bar has a smaller M/L ratio compared to that of the surrounding regions.

7.5 Irregular Galaxies: Interacting and Merging

Rotation curves for irregular galaxies are not straightforward. Some irregular galaxies exhibit quite normal rotation curves, such as observed for a ring galaxy NGC 660, amorphous galaxy NGC 4631 and NGC 4945 (Sofue et al. 1999a).

The interacting galaxy NGC 5194 (M51) shows a very peculiar rotation curve, which declines more rapidly than Keplerian at $R \sim 8 - 12$ kpc. This may

be due to inclination varying with the radius, e.g. warping. Because the galaxy is viewed nearly face-on ($i = 20^\circ$), a slight warp causes a large error in deriving the rotation velocity. If the galaxy's outer disk at 12 kpc has an inclination as small as $i \sim 10^\circ$, such an apparently steep velocity decrease would be observed even for a flat rotation.

When galaxies gravitationally interact, they tidally distort each other, and produce the pathological specimens that had until recently defied classification. In an innovative paper, Toomre (1977; see also Toomre & Toomre 1972; Holmberg 1941) arranged eleven known distorted galaxies “in rough order of completeness of the imagined mergers” starting with the Antennae (NGC 4038/39) and ending with NGC 7252. Observers rapidly took up this challenge, and Schweizer (1982) showed that NGC 7252 is a late-stage merger, in which the central gas disks of the two original spirals still have separate identities.

There is now an extensive literature both observational and computational (Schweizer 1998 and references therein; Barnes & Hernquist 1992, 1996; Hibbard et al. 2000) that make it possible to put limits on the initial masses, the gas quantities, the time since the initial encounter, and the evolutionary history of the merger remnant. Equally remarkable, tidal tails can be used as probes of dark matter halos (Dubinski et al. 1999).

Many nearby galaxies are also products of mergers, and hence have been extensively studied. NGC 5128 (Cen A) has a long history of velocity observations, with few signs of being completely untangled yet ($H\alpha$ long slit, Graham 1979; $H\alpha$ Fabry-Perot, Bland-Hawthorn et al. 1997; CO, Phillips et al. 1987; HI, van Gorkom et al. 1990; PN, Hui et al. 1995).

The starburst dwarf galaxy NGC 3034 (M82) shows an exceptionally peculiar rotation property (Burbidge et al. 1964; Sofue et al. 1992). It has a normal steep nuclear rise and rotation velocities which have a Keplerian decline beyond the nuclear peak. This may arise from a tidal truncation of the disk and/or halo by an encounter with M81 (Sofue 1998).

The past and present history of the Milky Way and the Local Group is written in the warp of the Milky Way (Garcia-Ruiz et al. 2000), in the tidal disruption of the Sagittarius dwarf (Ibata et al. 1995), in the mean retrograde motion of the younger globular clusters (Zinn 1993), in the tidal streams in the halo (Lynden-Bell and Lynden-Bell, 1995), and in the orbits of the Magellanic Clouds and the Magellanic stream (Murai & Fujimoto 1980; Gardiner & Naguchi 1996). For an excellent discussion “Interactions and Mergers in the Local Group” with extensive references, see Schweizer (1998).

7.6 Polar Ring Galaxies

Polar ring galaxies provide an unique opportunity to probe the rotation and mass distribution perpendicular to galaxy disks, and hence the three dimensional distribution of the dark matter (Schweizer et al. 1983; Combes & Arnaboldi 1996; Sackett & Sparke 1990, et al 1994; van Driel et al. 1995). The conclusion of Schweizer et al. (1983) from emission line velocities, that the halo mass is more nearly circular than flattened, has been contested by Sackett & Sparke

(1990), based on both emission and absorption line data. However, the data are limited and velocity uncertainties are large, so the conclusions are not robust.

A major surprise comes from the study of the polar ring galaxy NGC 4650A. Arnaboldi et al. (1997; see also van Gorkom et al. 1987) discovered an extended HI disk *coplanar with the ring*, which twists from almost edge-on to more face-on at large radii. The K-band optical features and the HI velocities can be fit simultaneously with a model in which spiral arms are present in this polar disk. Hence the polar ring is a very massive disk. This result strengthens previous suggestions that polar ring galaxies are related to spirals (Arnaboldi et al. 1995; Combes & Arnaboldi 1996).

8 THE FUTURE

Most of what we know about rotation curves we have learned in the last fifty years, due principally to instrumental and computational advances. It is likely that these advances will accelerate in the future. We can look forward to an exciting future. Specifically,

1. Extinction-free rotation kinematics in the central regions will come from high- J CO line spectroscopy and imaging using ALMA, the Andes large mm- and sub-mm wave interferometer at 5000 m altitude. This array will produce high spatial (0.01 arcsec) and high velocity ($\delta V < 1 \text{ km s}^{-1}$) resolution.

2. Extinction-free measurements will also come from eight- and ten-meter class telescopes using Br γ , H₂ molecular, and other infrared lines in K-band and longer-wavelength spectroscopy.

3. VLBI spectroscopic imaging of maser sources will teach us more about super massive black holes and rotation and mass distribution in nuclear disks.

4. Rotation of the Galaxy, separately for the disk and bulge, will be directly measured from proper motions, parallaxes, and hence, distances, and radial velocities of maser sources using micro-arcsecond radio interferometry. VERA (VLBI Experiment for Radio Astrometry) will become a prototype. This facility will also derive an accurate measurement of the Galactic Center distance, R_0 .

5. Optical interferometry may permit us to “watch” a nearby spiral (M31, M33, LMC, etc.) rotate on the plane of the sky, at least through a few microarcsecond. Radio interferometry of maser stars will be used to directly measure rotation on the sky of the nearest galaxies, from measures of proper motion (hence, distances) and radial velocities.

6. Rotation curves will be determined for galaxies at extremely high redshift; with luck we will observe protogalactic rotation and dynamical evolution of primeval galaxies. This may be a task for successive generations of space telescopes.

7. We may be lucky and ultimately understand details of barred spiral velocity fields from spectroscopic imaging. We may be able to separate the disk, bulge and bar potentials by fitting the number of parameters necessary for describing bar’s mass and dynamical properties.

8. Polar ring kinematics will be understood, especially halo kinematics perpendicular to the disk, and therefore, 3-D halo structure. We are certain to learn details of galaxies which are unexpected and hence surprising. We may even be luckier and learn something new about the Universe.

9. Sophisticated methods of analysis, perhaps involving line shapes and velocity dispersions, will produce more accurate rotation curves for large samples of spirals. These will lead to more tightly constrained mass deconvolutions. Distribution of dark and luminous matters within the halo, disk, bulge, and core will be mapped in detail from more sophisticated mass-to-luminosity ratio analyses.

10. Dark halos will finally be understood. We will know their extent, and their relation to the intracluster dark mass. We may even know the rotation velocity of the halo. Will the concept of a “rotation curve” apply at such large distances from the disk? Will we learn if our halo brushes the halo of M31?

11. We will ultimately know what dark matter is, the major constituent of the Universe when measured in mass. Elementary particle physics will teach us its origin and physical properties.

12. Perhaps we will be able to put to rest the last doubt about the applicability of Newtonian gravitational theory on a cosmic scale, or enthusiastically embrace its successor.

Acknowledgements: The authors thank Dr. Yoichi Takeda for assisting in gathering and selecting the references from a huge number of related papers in the decades. They thank Drs. Linda Dressel, Jeffrey Kenney, Stacy McGaugh, and Rob Swaters for references and helpful comments. They also thank Mareki Honma for references, Jin Koda and Kotaro Kohno for NMA data analyses.

This is an unedited draft of a chapter submitted for publication in the Annual Review of Astronomy and Astrophysics, Volume 39, 2001 (<http://astro.annualreviews.org/>).

References

- Aaronson M, Huchra J, Mould J 1980. *Ap. J.* 237:655
- Aaronson M, Mould J. 1986. *Ap. J.* 303:1
- Ables JG, Forster JR, Manchester RN, Rayner PT, Whiteoak JB, Mathewson DS, Kalnajs AJ, Peters WL, Wehner H. 1987. *MNRAS.* 226:157
- Amram P, Balkowski C, Boulesteix J, Cayatte V, Marcelin M, Sullivan III WT. 1996. *Astron. Astrophys.* 310:737
- Amram P, Boulesteix J, Marcelin M, Balkowski C, Cayatte V, Sullivan III WT. 1995. *Astron. Astrophys. Supp.* 113:35
- Amram P, Le Coarer E, Marcelin M, Balkowski C, Sullivan III WT, Cayatte V. 1992. *Astron. Astrophys. Supp.* 94:175
- Amram P, Marcelin M, Balkowski C, Cayatte V, Sullivan III WT, Le Coarer E. 1994. *Astron. Astrophys. Supp.* 103:5 year?
- Amram P, Sullivan III WT, Balkowski C, Marcelin M, Cayatte V. 1993. *Ap. J. Lett.* 403:59
- Argyle E. 1965. *Ap. J.* 141:750
- Arnabaldi M, Oosterloo T, Combes F, Freeman KC, Koribalski B. 1997. *Astron. J.* 113:585
- Arnabaldi M, Freeman KC, Gerhard O, Matthias M, Kudritzki RP, Mendez RH, Capaccioli M, Ford H. 1998. *Ap. J.* 507:759
- Arnabaldi M, Freeman KC, Sackett PD, Sparke LS, Capaccioli M. 1995. *Planetary & Sp. Sci.* 43:1377
- Ashman KM. 1992. *PASP. Ap. J.* 104:1109
- Athanassoula E Bureau 1999. *Ap. J.* 522:699
- Athanassoula E, Bosma A, Papaioannou S. 1987. *Astron. Astrophys. Supp.* 179:23
- Babcock HW. 1939. *Lick Obs. Bull.* 19:41
- Baldwin JE, Lynden-Bell D, Sancisi R. 1980. *MNRAS.* 193:313
- Bally J, Stark AA, Wilson RW, Henkel C. 1987. *Ap. J. Suppl.* 65:13
- Barnes JE, Hernquist L. 1992. *Annu. Rev. Astron. Astrophys.* 30:705
- Barnes JE, Hernquist L. 1996. *Ap. J.* 471:115
- Barteldrees A, & Dettmar R-J. 1994. *Astron. Astrophys. Suppl.* 103: 475
- Barton EJ, Bromley BC, Geller MJ. 1999. *Ap. J. Lett.* 511:25
- Begeman KG, Broeils AH, Sanders RH. 1991. *MNRAS.* 249:523
- Begeman KG. 1989. *Astron. Astrophys.* 223:47
- Bender R, Burstein D, Faber SM. 1992. *Ap. J.* 411:153.
- Bender R. 1990. *Astron. Astrophys.* 229:441
- Bershady MA, Haynes MP, Giovanelli R, Andersen DR. 1999. in *Galaxy Dynamics*. eds. DR Merritt, JA Sellwood, M Valluri. 182:263. San Francisco: Astron. Soc. Pacific
- Bershady MA. 1997. in *Dark Matter in the Universe*. eds. M Persic, P Salucci. 117:537. San Francisco: Astron. Soc. Pacific
- Bertola F, Bettoni D, Buson LM, Zeillinger WW. 1990. In *Dynamics and Interactions of Galaxies*. eds. ER Weilen. 249. Springer: Heideberg
- Bertola F, Bettoni D, Zeillinger WW. 1992. *Ap. J. Lett.* 401:79
- Bertola F, Cappellari M, Funes JG, Corsini EM, Pizzella A, Vega Bertran JC.

1998. *Ap. J. Lett.* 509:93
- Bertola F, Cinzano P, Corsini EM, Pizzella A, Persic M, Salucci P. 1996. *Ap. J. Lett.* 458:L67
- Bertola F, Galletta G. 1978. *Ap. J. Lett.* 226:115
- Binney J, Gerhard OE, Stark AA, Bally J, Uchida KI 1991. *MNRAS.* 252:210
- Binney J, Merrifield M. 1998. *Galactic Astronomy.* Princeton Univ. Press
- Binney J, Tremaine S. 1987. *Galactic Dynamics.* Princeton Univ. Press
- Binney J. 1982. *Annu. Rev. Astron. Astrophys.* 20:399
- Blais-Ouellette S, Amram P, Carignan C. 2000b. *Astron. J.* submitted.
- Blais-Ouellette S, Carignan C, Amram P, Cote S. 2000a. *Astron. J.* in press
- Bland-Hawthorn J, Freeman KC, Quinn PJ. 1997. *Ap. J.* 490:143
- Blitz L. 1979. *Ap. J.* 227:152
- Bosma A, van der Hulst JM, Athanassoula E, 1988. *Astron. Astrophys* 198:100
- Bosma A. 1981a. *Astron. J.* 86:1825
- Bosma A. 1981b. *Astron. J.* 86:1791
- Bosma A. 1996. in *Barred Galaxies.* eds. R Buta, DA Crocker, BG Elmegreen. *PASP Conf. Series.* 91:132.
- Brand J, Blitz L. 1993. *Astron. Astrophys.* 275:67.
- Braun R, Walterbos RAM, Kennicutt JR, Tacconi LJ. 1994. *Ap. J.* 420:558
- Brinks E, Skillman ED, Terlevich RJ, Terlevich E. 1997. *ApSS.* 248:23
- Broeils AH. 1992. *Astron. Astrophys.* 256:19
- Burbidge EM, Burbidge G. R. 1960. *Ap. J.* 132:30
- Burbidge EM, Burbidge GR, Crampin DJ, Rubin VC, Prendergast KH. 1964. *Ap. J.* 139:1058
- Burbidge EM, Burbidge GR. 1975. in *Stars and Stellar Systems IX: Galaxies and the Universe.* eds. A Sandage, M Sandage, J Kristian. University of Chicago Press, p. 81
- Bureau M, Athanassoula E. 1999. *Ap. J.* 522:686
- Burstein D, Bender R, Faber SM, Nolthenius R. 1997. *Astron. J.* 114:4
- Burstein D, Rubin VC, Ford Jr WK, Whitmore BC. 1986. *Ap. J. Lett.* 305:11
- Burton WB, Gordon MA. 1978. *Astron. Astrophys.* 63:7
- Buta R, Crocker DA, Elmegreen BG. 1996. eds. *Barred Galaxies.* PASJ Conf. Series. 91
- Buta R, Purcell GB, Cobb ML, Crocker DA, Rautiainen P, Salo H. 1999. *Astron. J.* 117:778
- Buta R, van Driel W, Braine J, Combes F, Wakamatsu K, Sofue Y, Tomita A. 1995 *Ap. J.* 450:593
- Cayatte V, van Gorkom JM, Balkowski C, Kotanyi C. 1990. *Astron. J.* 100:604
- Carignan C, Beaulieu S. 1989. *Ap. J.* 347:760
- Carignan C, Freeman KC. 1985. *Ap. J.* 294:494
- Carignan C, Puche D. 1990. *Astron. J.* 100:394
- Carignan C, Puche D. 1990. *Astron. J.* 100:641
- Carignan C. 1985. *Ap. J.* 299:59
- Carter D, Jenkins CR. 1993. *MNRAS.* 263:1049
- Casertano S, van Gorkom JH. 1991. *Astron. J.* 101:1231
- Casertano S. 1983. *MNRAS.* 203:735

- Clemens, DP. 1985. *Ap. J.* 295:422
- Combes F, 1992. *Annu. Rev. Astron. Astrophys.* 29:195
- Combes F, Arnaboldi M. 1996. *Astron. Astrophys.* 305:763
- Combes F, Mamon GA, Charmandaris V. 2000. eds. *Dynamics of Galaxies: from the Early Universe to the Present (XVth IAP Meeting: PASP. Conf. Series)*. Vol. 197
- Corradi RLM, Boulesteix J, Bosma A, Amram P, Capaccioli M. 1991. *Astron. Astrophys.* 244:27
- Courteau, S. 1997. *Astron. J.* 114:2402
- Courteau, S, Rix, HW. 1999 *Ap. J.* 513:561
- de Blok E, McGaugh, SS, Rubin VC. 2001. in *Galaxy Disks and Disk Galaxies*. eds. J Funes, E Corsini. *PASP. Conf. Series*, in press
- de Blok WJG, McGaugh SS, van der Hulst JM. 1996. *MNRAS* 283:18
- de Blok WJG, McGaugh SS. 1998. *Ap. J.* 508:132
- de Vaucouleurs G, Freeman KC. 1973. *Vistas in Astronomy*. 14:163
- de Vaucouleurs G. 1959. in *Handbuch der Physics, Astrophysik IV* 53:310
- de Zeeuw T, Franx M. 1991. *Annu. Rev. Astron. Astrophys.* 29:239
- Deguchi S, Fujii T, Izumiura H, Kameya O, Nakada Y, Nakashima J, Ootsubo T, Ukita N. 2000. *Ap. J. Suppl.* 128:571
- Dressler A. 1984. *Annu. Rev. Astron. Astrophys.* 22:185
- Dubinski J, Mihos JC, Hernquist L. 1999. *Ap. J.* 526:607
- Einasto J, Saar E, Kaasik A, Chernin AD. 1974. *Nature*. 252:111
- Evans NW, Collett JL. 1994. *Ap. J. Lett.* 420:67
- Faber SM, Gallagher JS. 1979. *Annu. Rev. Astron. Astrophys.* 17:135
- Ferrarese L, Ford HC. 1999. *Ap. J.* 515:583
- Fich M, Blitz L, Stark A. 1989. *Ap. J.* 342:272
- Fischer P. et al. 2000. *Astron. J.* submitted
- Fisher D. 1997. *Astron. J.* 113:950
- Forbes, DA. 1992. *Astron. Astrophys. Supp.* 92:583
- Franx M, Illingworth GD, de Zeeuw T. 1991. *Ap. J.* 383:112
- Franx M, Illingworth GD. 1988. *Ap. J. Lett.* 327:55
- Fraternali F, Oosterloo T, Sancisi R, van Moorsel G. 2000. in *Gas and Galaxy Evolution, VLA 20th Anniversary Conference*, J.E. Hibbard, M.P. Rupen & J.H. van Gorkom (eds.), in press
- Funes SJ, Corsini EM. 2001. eds. *Galaxy Disks and Disk Galaxies (ASP. Conf. Series)* in press
- Galletta G. 1987. *Ap. J.* 318:531
- Galletta G. 1996. in *Barred Galaxies*. eds. R Buta, DA Crocker, Elmegreen BG. *PASP. Conf. Series*. 91:429
- Garcia-Burillo S, Guélin M, Cernicharo J. 1993. *Astron. Astrophys.* 274:123
- Garcia-Burillo S, Sempere MJ, Bettoni D. 1998. *Ap. J.* 502:235
- Garcia-Ruiz I, Kuijken K, Dubinski J. 2000. *MNRAS*. submitted
- Gardiner LT, Noguchi M. 1996. *MNRAS*. 278:191
- Genzel R, Eckart A, Ott T, Eisenhauer F. 1997. *MNRAS*. 291:219
- Genzel R, Pichon C, Eckart A, Gerhard OE, Ott T. 2000. *MNRAS*. 317:348
- Gerhard OE. 1993. *MNRAS*. 265:213

- Gerssen J. 2000. thesis Rijksuniversiteit Groningen
 Ghez A, Morris M, Klein BL, Becklin EE. 1998. *Ap. J.* 509:678.
 Gilmore G, King IR, van der Kruit PC. 1990. in *The Milky Way as a Galaxy*.
 University Science Books: Mill Valley, CA
 Graham JA. 1979. *Ap. J.* 232:60
 Greenhill LJ, Gwinn CR, Antonucci R, Barvainis R. 1996. *Ap. J. Lett.* 472:L21
 Greenhill LJ, Moran JM, Herrnstein JR. 1997. *Ap. J. Lett.* 481:L23
 Guhathakrta P, van Gorkom JH, Kotanyi CG, Balkowski C. 1988. *Astron. J.*
 96:851
 Héraudeau Ph, Simien F. 1997. *Astron. Astrophys.* 326:897
 Handa T, Nakai N, Sofue Y, Hayashi M, Fujimoto M, 1990. *Publ. Astron. Soc.*
Jaapn. 42:1
 Haschick AD, Baan WA, Schneps MH, Reid MJ, Moran JM, Guesten R. 1990.
Ap. J., 356:149.
 Haynes MP, Hogg DE, Maddalena RJ, Roberts MS, van Zee L. 1998. *Astron.*
J. 115:62
 Heisler J, Merritt D, Schwarzschild M. 1982. *Ap. J.* 258:490
 Héraudeau P, Simien F. 1997. *Astron. Astrophys.* 326:897
 Hernquist L, Barnes JE. 1991. *Nature.* 354:10
 Herrnstein JR, Moran JM, Greenhill LJ, Diamond PJ, Inoue M, Nakai N,
 Miyoshi M, Henkel C, Riess A. 1999. *Nature.* 400:539
 Hibbard JE, Vacca WD, Yun MS. 2000. *Astron. J.* 119:1130
 Hoekstra H. 2000. thesis Rijksuniversiteit Groningen
 Holmberg E. 1941. *Ap. J.* 94:385
 Honma M, Sofue Y, Arimoto N. 1995. *Astron. Astrophys.* 304:1
 Honma M, Sofue Y. 1996. *Publ. Astron. Soc. Japan Lett.* 48:103.
 Honma M, Sofue Y. 1996. *Publ. Astron. Soc. Japan Lett.* 48:103
 Honma M, Sofue Y. 1997a. *Publ. Astron. Soc. Japan.* 49:453
 Honma M, Sofue Y. 1997b. *Publ. Astron. Soc. Japan.* 49:539
 Hui X, Ford HC, Freeman KC, Dopita MA. 1995. *Ap. J.* 449:592
 Hunter DA, Rubin VC, Gallagher III, JS. 1986. *Astron. J.* 91:1086
 Hunter JH, Gottesman ST. 1996. in *Barred Galaxies*. eds. R Buta, DA Crocker,
 Elmegreen BG. *PASP. Conf. Series.* 91:398
 Ibata, RA, Gilmore G, Irwin MJ. 1995. *MNRAS.* 277:781
 Irwin JudithA, Sofue Y. 1992. *Ap. J. Lett.* 396:L75.
 Irwin JudithA, Seaquist ER. 1991. *Ap. J.* 371:111
 Ishizuki S, Kawabe R, Ishiguro M, Okumura SK, Morita KI, Chikada Y, Kasuga
 T, Doi M. 1990. *Ap.J.* 355:436
 Izumiura H, Deguchi S, Hashimoto O, Nakada Y, Onaka T, Ono T, Ukita N,
 Yamamura I. 1995. *Ap. J.* 453:837
 Izumiura H. Deguchi S, Fujii T, Kameya O, Matsumoto S, Nakada Y, Ootsubo
 T, Ukita N. 1999. *Ap. J. Suppl.* 125:257
 Jacoby GH, Ciardullo R, Ford HC. 1990. *Ap. J.* 356:332
 Jedrzejewski R, Schechter P. 1989. *Astron. J.* 98:147
 Jobin M, Carignan C. 1990. *Astron. J.* 100:648
 Kamphuis J, Briggs F. 1992. *Astron. Astrophys.* 253:335

- Kaneko N, Aoki K, Kosugi G, Ohtani H, Yoshida M, Toyama K, Satoh T, Sasaki M. 1997. *Astron. J.* 114:94
- Kannappan SJ, Fabricant DG. 2000. *Astron. J.* in press
- Kelson DD, Illingworth GD, van Dokkum PG, Franx M. 2000a. *Ap. J.* 31:159
- Kelson DD, Illingworth GD, van Dokkum PG, Franx M. 2000b. *Ap. J.* 531:184
- Kenney J, Young SJ 1988. *Astrophys. J. Suppl* 66:261
- Kenney JDP, Wilson CD, Scoville NZ, Devereux NA, Young JS. 1992. *Ap. J. L.* 395:L79
- Kenney JPD, Faundez. 2000. in *Stars, Gas and Dust in Galaxies: Exploring the Links. PASP. Conf. Series.* in press
- Kent SM. 1986. *Astron. J.* 91:1301
- Kent SM. 1987. *Astron. J.* 93:816.
- Kent SM. 1991. *Ap. J.* 378:131
- Kent SM. 1992. *Ap. J.* 387:181
- Kim S, Stavelly-Smith L, Dopita MA, Freeman KC, Sault RJ, Kesteven MJ, McConnell D. 1998. *Ap. J.* 503:674.
- Koda J, Sofue Y, Wada K. 2000a. *Ap. J.* 532:214
- Koda J, Sofue Y, Wada K. 2000b. *Ap. J. L.* 531:L17
- Kohno K, Kawabe R, Villa-Vilaro B. 1999.. *Ap. J.* 511:157
- Kohno K. 1998. PhD. Thesis, University of Tokyo
- Koo D. C. 1999. in *Proceedings of XIX Moriond Meeting on Building Galaxies: from the Primordial Universe to the Present.* eds. F Hammer, TX Thuan, V Cayatte, B Guiderdoni J, Tran Thanh Van (Gif-sur-Yvette: Editions Frontieres), in press
- Kormendy J, Richstone D. 1995. *Ann. Rev. Astron. Astrophys.* 33:581
- Kormendy J, Westpfahl DJ, 1989. *Ap. J.* 338:752
- Kormendy J. 1983. *Ap. J.* 275:529
- Kormendy J. 2001. in *Galaxy Disks and Disk Galaxies.* eds. J Funes, E Corsini. *PASP. Conf. Series,* in press
- Krabbe A, Colina L, Thatte N, Kroker H. 1997. *Ap. J.* 476:98
- Kuijken K, Merrifield MR. 1993. *MNRAS.* 264:712
- Kuijken K. 1996. *MNRAS.* 283:543
- Kuno N, Nishiyama K, Nakai N, Sorai K, Vila-Vilaro B. 2000. *Publ. Astron. Soc. japan.* 52:775
- Kyazumov GA, 1984. *AZh.* 61:846
- Lake G, Schommer RA, van Gorkom JH. 1990. *Astron. J.* 99:547
- Larkin JE, Armus L, Knop RA, Matthews K, Soifer BT. 1995. *Ap. J.* 452:599
- Lequeux J. 1983. *Astron. Astrophys.* 125:394
- Lin DNC, Pringle JE 1987. *Ap. J. L.* 320:L87
- Lindblad B. 1959. in *Handbuch der Physics, Astrophysik IV* 53:21
- Lindqvist M, Habing HJ, Winnberg A. 1992a. *Astron. Astrophys.* 259:118
- Lindqvist M, Winnberg A, Habing HJ, Matthews HE. 1992b. *Astron. Astrophys. Suppl.* 92:43
- Lynden-Bell D, Lynden-Bell RM. 1995. *MNRAS.* 275:429
- Maciejewski W, & Binney J. 2000. IAU Symposium No. 205. *Galaxies and their Constituents at the Highest Angular Resolution* in press

- Mathewson DS, Ford VL, Buchhorn M. 1992. *Ap. J. Suppl.* 81:413
- Mathewson DS, Ford VL. 1996. *Ap. J. Suppl.* 107:97
- Mayall NU. 1951. in *The Structure of the Galaxy*. Ann Arbor: University of Michigan Press p. 19
- McGaugh SS, & de Blok WJG. 1998. *Ap. J.* 499:66
- Mediavilla E, Arribas S, Garcia-Lorenzo B, Del Burgo C. 1998. *Ap. J.* 488:682
- Merrifield MR, Kuijken K. 1994. *Ap. J.* 432:75
- Merrifield MR. 1992. *Astron. J.* 103:1552.
- Merritt DR, Sellwood JA, Valluri M. 1999. eds. *Galaxy Dynamics*. San Francisco: Astron. Soc. Pacific
- Mestel L. 1963. *MNRAS.* 126:553
- Milgrom M, Braun E. 1988. *Ap. J.* 334:130
- Milgrom M. 1983. *Ap. J.* 270:371
- Miyoshi M, Moran J, Herrnstein J, Greenhill L, Nakai N, Diamond P, Inoue M. 1995. *Nature.* 373:127.
- Mo HJ, Mao S, White SDM. 1998. *MNRAS.* 295:319
- Moellenhoff C, Matthias M, Gerhard OE. 1995. *Astron. Astrophys.* 301:359
- Mulchaey JS, Regan MW. 1997. *Ap. J. Lett.* 482:L135
- Murai T, Fujimoto M 1980. *Publ. Astron. Soc. Japan.* 32:581
- Nakai N, Inoue M, Miyoshi M 1993. *Nature.* 361:45
- Nakai N, Kuno N, Handa T, Sofue Y. 1994. *Publ. Astron. Soc. Jpn.* 46:527
- Nelson AH. 1988. *MNRAS.* 233:115
- Nishiyama K, Nakai N. 1998. IAU Symposium No. 184 *The central regions of the Galaxy and galaxies* p.245
- Noguchi N. 1988. *Astron. Astrophys.* 203:259
- Oestlin G, Amram P, Masegosa J, Bergvall N, Boulesteix J. 1999. *Astron. Astrophys. Supp.* 137:419
- Oka T, Hasegawa T, Sato F, Tsuboi M, Miyazaki A, 1998. *Ap.J.S.* 118:455
- Oort JH. 1940. *Ap. J.* 91:273
- Ostriker JP, Peebles PJE. 1973. *Ap. J.* 186:467
- Ostriker, JP, Peebles, PJE, Yahil A. 1974. *Ap. J.* 193:L10
- Page T. 1952. *Ap. J.* 116:63 erratum 136:107
- Pease FG. 1918. *Proc. Nat. Acad. Sci. US* 4:21
- Peebles PJE. 1995. *Ap. J.* 449:52
- Persic M, Salucci P, Stel F. 1996. *MNRAS.* 281:27
- Persic M, Salucci P. 1988. *MNRAS.* 234:31
- Persic M, Salucci P. 1990a. *MNRAS.* 247:349
- Persic M, Salucci P. 1990b. *MNRAS.* 245:577
- Persic M, Salucci P. 1995. *Ap. J. Supp.* 99:501
- Persic M, Salucci P. 1997. eds. *Dark Matter in the Universe*. San Francisco: Astron. Soc. Pacific
- Peterson CJ, Rubin VC, Ford Jr WK, Thonnard N. 1978. *Ap. J.* 219:31
- Phillips TG, Ellison BN, Keene JB, Leighton RB, Howard RJ, Masson CR, Sanders DB, Veidt B, Young K. 1987. *Ap. J. Lett.* 322:L73
- Plummer HC. 1911. *MNRAS.* 71:460
- Prada, F, Gutierrez CM, Peletier RF, McKeith CD. 1996. *Ap. J.* 463:9

- Puche D, Carignan C, Bosma A. 1990. *Astron. J.* 100:1468
- Puche D, Carignan C, Wainscoat RJ. 1991a. *Astron. J.* 101:447
- Puche D, Carignan C, van Gorkom JH. 1991b. *Astron. J.* 101:456
- Regan MW, Vogel SN. 1994. *Ap. J.* 43:536
- Richstone D, Bender R, Bower G, Dressler A, Faber S, et al. 1998. *Nature* 395A:14 .
- Richter O-G, Sancisi R. 1994. *Astron. Astrophys.* 290:19
- Rix H-W, Carollo CM, Freeman K. 1999. *Ap. J. Lett.* 513:L25
- Rix H-W, Franx M, Fisher D, Illingworth G. 1992. *Ap. J. Lett.* 400:5
- Rix H-W, Kennicutt RC, Braun R, Walterbos RAM. 1995. *Ap. J.* 438:155
- Rix H-W, White S. 1992. *MNRAS.* 254:389
- Rix H-W, de Zeeuw PT, Cretton N, van der Marel RP, Carollo CM. 1997. *Ap. J.* 488:702
- Roberts MA, Rots AH. 1973. *Astron. Astrophys.* 26:483.
- Roelfsema PR, Allen RJ. 1985. *Astron. Astrophys.* 146:213
- Rogstad DH, Shostak GS. 1972. *Ap. J.* 176:315
- Roscoe DF. 1999. *Astron. Astrophys.* 343:788
- Rubin VC, Burbidge EM, Burbidge GR, Prendergast KH. 1965. *Ap. J.* 141:885.
- Rubin VC, Burstein D, Ford Jr WK, Thonnard N. 1985. *Ap. J.* 289:81
- Rubin VC, Ford Jr WK, Thonnard N. 1980. *Ap. J.* 238:471
- Rubin VC, Ford Jr WK, Thonnard N. 1982. *Ap. J.* 261:439
- Rubin VC, Ford Jr WK. 1970. *Ap. J.* 159:379
- Rubin VC, Ford Jr WK. 1983. *Ap. J.* 271, 556R
- Rubin VC, Graham JA, Kenney JD. 1992. *Ap. J. Lett.* 394:9
- Rubin VC, Graham JA. 1987. *Ap. J. Lett.* 316:67
- Rubin VC, Hiltiwanger, J. 2001. in *Galaxy Disks and Disk Galaxies.* eds. J Funes, E Corsini. *PASP. Conf. Series*, in press
- Rubin VC, Hunter DA, Ford Jr WK. 1991. *Ap. J. Supp.* 76:153
- Rubin VC, Hunter DA. 1991. *Ap. J. Supp.* 76:153
- Rubin VC, Kenney JD, Boss AP, Ford Jr WK. 1989. *Astron. J.* 98:1246
- Rubin VC, Kenny JDP, Young, JS. 1997. *Astron. J.* 113:1250
- Rubin VC, Thonnard N, Ford Jr WK. 1982. *Astron. J.* 87:477
- Rubin VC, Thonnard N, Ford WK Jr. 1978. *Ap. J. Lett.* 225:L107
- Rubin VC, Waterman AH, Kenney JD, 1999. *Astron. J.* 118:236
- Rubin VC, Whitmore B C, Ford Jr W K, 1988. *Ap. J.* 333:522
- Rubin VC. 1994a. *Astron. J.* 107:173
- Rubin VC. 1994b. *Astron. J.* 108:456
- Rubin VC. 1987. in *Observational Evidence of Activity in Galaxies.* eds. EYe Khachikian, KJ Fricke, & J Melnick. I.A.U. Symposium 121:461. Reidel:Dordrecht
- Sackett PD, Rix H-W, Jarvis BJ, Freeman KC. 1994. *Ap. J.* 436:629
- Sackett PD, Sparke LS, 1990. *Ap. J.* 361:408
- Sackett PD, Sparke LS. 1994. or et al
- Sakamoto K, Okumura SK, Ishizuki S, Scoville NZ 1999. *Ap.J. S.* 124:403
- Salo H, Rautiainen P, Buta R, Purcell GB, Cobb ML, Crocker DA, Laurikainen E. 1999. *Astron. J.* 117:792.

- Salucci P, Ashman KM, Persic M. 1991. *Ap. J.* 379:89
- Salucci P, Frenk CS. 1989. *MNRAS.* 237:247
- Sancisi R, Allen RJ, Sullivan III WT. 1979. *Astron. Astrophys.* 78:217
- Sancisi R. 2001. in *Galaxy Disks and Disk Galaxies.* eds. J Funes, E Corsini. *PASP. Conf. Series*, in press
- Sanders RH, Verheijen MAW. 1998. *Ap. J.* 503:97
- Sanders, RH. 1996. *Ap. J.* 473:117
- Sargent AI, Welch WJ. 1993. *Annu. Rev. Astron. Astrophys.* 31:297.
- Sargent WLW, Schechter PL, Boksenberg A, Shortridge K. 1977. *Ap. J.* 212:326
- Sawada-Satoh S, Inoue M, Shibata KM, Kameno S, Migenes V, Nakai N, Diamond PJ. 2000. *Publ. Astron. Soc. Jpn.* 52:421
- Schaap WE, Sancisi R, Swaters RA 2000. *Astron. Astrophys. L.* 356:49
- Schinnerer E, Eckart A, Tacconi LJ, Genzel R, Downes D. 2000. *Ap. J.* 533:850.
- Schombert JM, Bothun GD, Schneider SE, McGaugh SS. 1992. *Astron. J.* 103:1107
- Schombert JM. Bothun GD. 1988. *Astron. J.* 95:1389
- Schwarzschild M. 1954. *Astron. J.* 59:273
- Schweizer F, Whitmore BC, Rubin VC. 1983. *Astron. J.* 88:909
- Schweizer F. 1982. *Ap. J.* 252:455
- Schweizer F. 1998. in *Galaxies: Interactions and Induced Star Formation*, Swiss Society for Astrop. Astron. XIV, eds. R. C. Kennicutt, Jr. F. Schweizer, J. E. Barnes, D. Friedli, L. Martinet, & D. Pfenniger. Springer-Verlag Berlin
- Scoville NZ, Thakker D, Carlstrom JE, Sargent AE 1993. *Ap. J. L* 404:L63
- Shlosman I, Begelman MC, Frank, J 1990. *Nature.* 345:679
- Sjouwerman LO, van Langevelde HJ, Winnberg A, Habing HJ. 1998. *Astron. Astrophys. Suppl.* 128:35
- Sil'chenko KO. 1996. *Ast. L.* 22:108
- Simard L, Prichet CJ. 1998. *Ap. J.* 505:96
- Simkin SM. 1974. *Astron. Astrophys.* 31:129
- Slipher VM. 1914. *Lowell Obs. Bull.* 62
- Sofue Y, Honma M, Arimoto N. 1995. *Astron. Astrophys.* 296:33
- Sofue Y, Irwin JudithA. 1992. *Publ. Astron. Soc. Jpn.* 44:353
- Sofue Y, Koda J, Kohno K, Okumura SK, Honma M, Kawamura A, Irwin JudithA. 2000. *Ap. J. Lett.* in press.
- Sofue Y, Reuter H-P, Krause M, Wielebinski R, Nakai N. 1992. *Ap. J.* 395:126
- Sofue Y, Tomita A, Honma M, Tutui Y, Takeda Y. 1998. *Publ. Astron. Soc. Japan.* 50:427
- Sofue Y, Tomita A, Honma M, Tutui Y. 1999b. *Publ. Astron. Soc. Jpn.* 51:737
- Sofue Y, Tutui Y, Honma M, Tomita A, Takamiya T, Koda J, Takeda Y. 1999a. *Ap. J.* 523:136
- Sofue Y, Tutui Y, Honma M, Tomita A. 1997. *Astron. J.* 114:2428
- Sofue Y. 1995. *Publ. Astron. Soc. Jpn.* 47:527
- Sofue Y. 1996. *Ap. J.* 458:120
- Sofue Y. 1997. *Publ. Astron. Soc. Japan.* 49:17
- Sofue Y. 1998. *Publ. Astron. Soc. Japan.* 50:227
- Sofue Y. 1999. *Publ. Astron. Soc. Japan.* 51:445

- Sorai K, Nakai N, Kuno N, Nishiyama K, Hasegawa T. 2000. *Publ. Astron. Soc. Japan.* 52:785
- Sorensen S-A, Matsuda T, Fujimoto M. 1976. *Astrophys. Sp. Sci.* 43:491
- Sperandio M, Chincarini G, Rampazzo R, de Souza R. 1995. *Astron. Astrophys. Supp.* 110:279
- Sridhar S, Touma J. 1996. *MNRAS.* 279:1263
- Steinmetz M, Navarro JF. 1999. *Ap. J.* 513:555
- Swaters RA, Madore BF, Trewhella M. 2000. *Ap. J. Lett.* 356:L49.
- Swaters RA, Sancisi R, van der Hulst JM. 1997. *Ap. J.* 491:140
- Swaters RA, Schoenmakers RHM, Sancisi R, van Albada TS. 1999. *MNRAS.* 304:330
- Swaters RA. 1999. thesis Rijksuniversiteit Groningen
- Swaters RA. 2001. in *Galaxy Disks and Disk Galaxies.* eds. J Funes, E Corsini. *PASP. Conf. Series*, in press
- Takamiya T, Sofue Y. 2000. *Ap. J.* 534:670
- Tecza M, Thatte N, Maiolino R. 2000. IAU Symposium No. 205. *Galaxies and their Constituents at the Highest Angular Resolution* in press
- Thaker AR, Ryden BS. 1998. *Ap. J.* 506:93
- Toomre A, Toomre J. 1972. *Ap. J.* 178:623
- Toomre A. 1977. in *The Evolution of Galaxies and Stellar Populations.* eds. BM Tinsley, RB Larson. Yale University Observatory
- Toomre A. 1982. *Ap. J.* 259:535
- Tremaine S, Yu Q. 2000. *MNRAS.* submitted
- Trimble V. 1987. *Annu. Rev. Astron. Astrophys.* 25:425
- Trotter AS, Greenhill LJ, Moran JM, Reid MJ, Irwin JudithA, Lo K-Y. 1998. *Ap. J.* 495:740
- Tully RB, Fisher JR. 1977. *Astron. Astrophys.* 54:661
- Tully RB, Bottinelli L, Fisher JR, Goughenheim L, Sancisi R, van Woerden H. 1978. *Astron. Astrophys.* 63:37
- Valluri M. 1993. *Ap. J.* 408:57
- Valluri M. 1994. *Ap. J.* 430:101
- van Albada TS, Bahcall JN, Begeman K, Sancisi R. 1985. *Ap. J.* 295:305
- van Albada TS, Kotanyi CG, Schwarzschild M. 1982 *MNRAS.* 198:303
- van Driel W, Combes F, Casoli F, Gerin M, Nakai N, Miyaji T, Hamabe M, Sofue Y, Ichikawa T, Yoshida S, Kobayashi Y, Geng F, Minezaki T, Arimoto N, Kodama T, Goudfrooij P, Mulder PS, Wakamatsu K, Yanagisawa K. 1995. *Astron. J.* 109:942
- van Gorkom JH, Schechter PL, Kristian J. 1987. *Ap. J.* 314:457
- van Gorkom JH, van der Hulst JM, Haschick AD, Tubbs AD. 1990. *Astron. J.* 99:1781
- van Moorsel GA. 1983. *Astron. Astrophys. Supp.* 54:1
- van de Hulst HC, Raimond E, van Woerden H. 1957. *Bull. Ast. Inst. Neth.* 14:1
- van der Kruit PC, Allen RJ. 1978. *Annu. Rev. Astron. Astrophys.* 16:103
- van der Kruit PC. 2001. in *Galaxy Disks and Disk Galaxies.* eds. J Funes, E Corsini. *PASP. Conf. Series*, in press

- van der Marel M, Franx M. 1993. *Ap. J.* 407:525
- van der Marel RP, Rix HW, Carter D, Franx M, White SDM, de Zeeuw T. 1994. *MNRAS.* 268:521
- Vaughan JM. 1989. *The Fabry-Perot interferometer. History, theory, practice and applications.* The Adam Hilger Series on Optics and Optoelectronics, Bristol: Hilger.
- Vega Baltran JC. 1999. Thesis Universidad de La Laguna
- Verheijen MAW. 1997. thesis Rijksuniversiteit Groningen
- Vogel SN, Rand RJ, Gruend RA, Teuben PJ. 1993. *PASP.* 105:666
- Vogt NP, Forbes DA, Phillips AC, Gronwall C, Faber SM, Illingworth GD, Koo DC. 1996. *Ap. J. Lett.* 465:15
- Vogt NP, Herter T, Haynes MP, Courteau S. 1993. *Ap. J. Lett.* 415:95V
- Vogt NP, Phillips AC, Faber SM, Gallego J, Gronwall C, Guzman R, Illingworth GD, Koo DC, Lowenthal J D. et al. 1997. *Ap. J. Lett.* 479:121
- Volders L. 1959. *BAN.* 1:323
- Wada K, Habe A 1992. *MNRAS.* 258:82
- Wada K, Habe A 1995. *MNRAS.* 277:433
- Wada K, Sakamoto K, Minezaki T. 1998. *Ap.J.* 494:236
- Walterbos RAM, Braun R, Kennicutt Jr RC. 1994. *Astron. J.* 107:184
- Warner PJ, Wright MCH, Baldwin JE. 1973, *MNRAS.* 163:163
- Watson WD, Wallim BK. 1994. *Ap. J.* 432:35
- Weiner B, Sellwood JA. 1999. *Ap. J.* 524:112
- Weiner BJ, Williams TB. 1996. *Astron. J.* 111:1156
- Weiner BJ, Williams TB, van Gorkom JH, Sellwood SA. 2000. *Ap. J.* accepted.
- Weiner BJ, Sellwood SA, Williams TB. 2000. *Ap. J.* accepted.
- Westerlund BE. 1999. in *New Views of the Magellanic Clouds*, IAU Symposium No. 190, eds Y.-H. Chu, N. Suntzeff, J. Hesser, & D. Bohlender. in press
- Whitmore BC, Forbes DA, Rubin VC. 1988. *Ap. J.* 333:542
- Whitmore BC, Forbes DA. 1989. *ApSS.* 156:175
- Wilkinson MI, & Evans NW. 1999. *MNRAS.* 310:645
- Wolf M. 1914. *Vierteljahresschr Astron. Ges.* 49:162
- Woods D, Madore BF, Fahlman GG. 1990. *Ap. J.* 353:90
- Wozniak H, Pfenniger D. 1997. *Astron. Astrophys.* 317:14
- Young JS, Xie S, Tacconi L, Knezek P, Vicuso P, Tacconi-Garman L, Scoville N, Schneider S, et al. 1995. *Ap. J. Suppl* 98:219
- Young JS, Scoville NZ. 1992. *Ann. Rev. Astron. Astrophys.* 29:581
- Zaritsky D, Elston R, Hill JM. 1989. *Astron. J.* 97:97
- Zaritsky D, Elston R, Hill JM. 1990. *Astron. J.* 99:1108
- Zaritsky D, White SDM. 1994. *Ap. J.* 435:599
- Zaritsky D. 1992. *Publ. Astron. Soc. Pac.* 104:831
- Zinn R. 1993. in *The globular clusters-galaxy connection.* ASP Conf. Series. eds. Graeme H. Smith, and Jean P. Brodie. 48:38